

TABLE 1

## AGS cDNAs isolated from cardiac hypertrophy model of mouse

AGSs are numbered according to the order in which they were isolated from a functional screen in yeast. GPR, G-protein-regulatory motif. The number of transformants screened for each cDNA library of the heart is as follows: transverse aortic constriction,  $1.6 \times 10^7$ ; isoproterenol infusion,  $2.0 \times 10^7$ .

Gene in database	AGS	Cardiac dysfunction model used to generate cDNA libraries for functional screen <sup>a</sup>	
		Transverse aortic constriction	Isoproterenol infusion
<i>Dynl1b</i> (the entire coding sequence)	AGS2	+	—
<i>GPSM1</i> (C-terminal 178 amino acids with 3 GPR motifs)	AGS3	+	—
<i>RGS12</i> (C-terminal 206 amino acids with GPR motif)	AGS6	+	+
<i>TFE3</i> (C-terminal 533 amino acids)	AGS11	+	+
<i>TFEB</i> (C-terminal 320 amino acids)	AGS12	—	+
<i>MITF</i> (C-terminal 304 amino acids)	AGS13	+	+

<sup>a</sup> cDNA libraries were screened in yeast strains CY1141 ( $G\alpha_{13}$ ), CY8342 ( $G\alpha_s$ ), and CY9603 ( $G\alpha_{16}$ ).

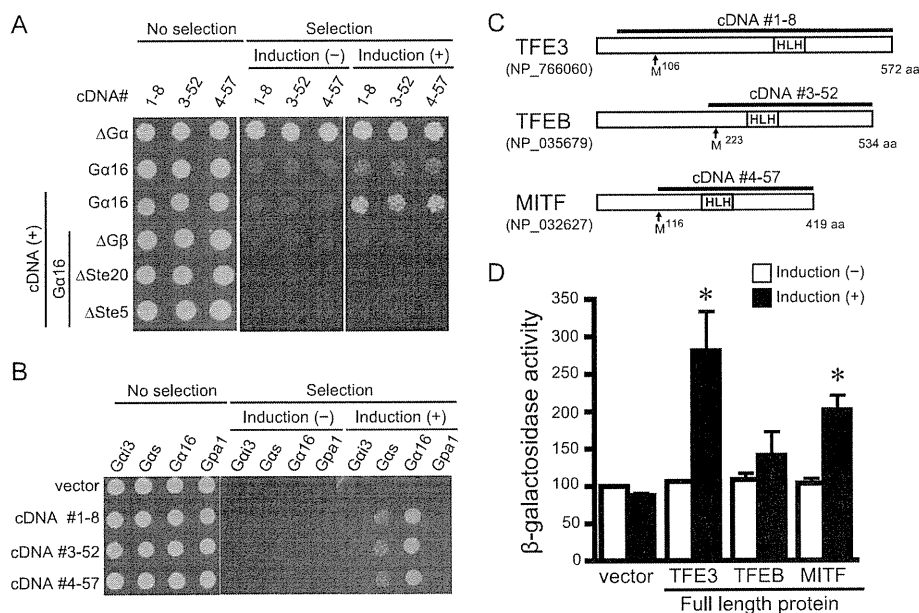


FIGURE 1. Bioactivity and diagram of AGSs isolated from mouse hypertrophic heart. In *A* and *B*, data are presented in three panels to illustrate the viability of the transformed yeast and the galactose-dependent growth under the selective pressure of exclusion of histidine from the medium. Galactose promotes the expression of each cDNA in the pYES2-containing *GAL1* promoter. About 2000 cells were suspended in H<sub>2</sub>O and spotted on medium with glucose plus histidine (*left*; no selection), glucose minus histidine (*center*; selection without induction), or galactose plus histidine (*right*; selection plus induction). *A*, epistasis analysis of isolated clones. Transformants in a yeast strain expressing human  $G\alpha_{16}$  (Gpa1(1–41)) and yeast lacking  $G\alpha$ ,  $G\beta$ , or downstream signaling molecules ( $\Delta G\alpha$ , yeast lacking  $G\alpha$ ;  $\Delta G\beta$ , yeast lacking  $G\beta$ ;  $\Delta Ste20$ , yeast lacking p21-activated kinase;  $\Delta Ste5$ , yeast lacking the kinase scaffold protein). *B*, effect of isolated cDNAs in yeast expressing various types of  $G\alpha$ . *C*, schematic diagram of the sequences of TFE3, TFEB, and MITF in mouse. The line above the sequence refers to cDNA isolated by the yeast-based functional screen. HLH, helix-loop-helix. *D*, bioactivity of full-length TFE3, TFEB, and MITF. The full-length clones were transformed into yeast expressing  $G\alpha_{16}$ . The magnitude of activation of G-protein signaling pathway was monitored by  $\beta$ -galactosidase activity. Data are presented as the mean S.E. of five experiments with duplicate determinations. \*,  $p < 0.05$  versus non-induction group.

## Miscellaneous Procedures and Statistical Analysis

Immunoblotting and data analysis were performed as described previously (18, 24). The luminescence images captured with an image analyzer (LAS-3000, Fujifilm, Tokyo, Japan) were quantified using Image Gauge 3.4 (Fujifilm). Data are expressed as mean  $\pm$  S.E. from independent experiments as described in the figure legends. Statistical analyses were performed using the unpaired *t* test, F-test, and one-way analysis of variance followed by Tukey's multiple comparison post hoc test. All statistical analyses were performed with Prism 4 (GraphPad Software).

## RESULTS

**Identification of Activators of G-protein Signaling from Hypertrophied Hearts**—We utilized an expression cloning system in *S. cerevisiae* to identify receptor-independent activators

of G-protein signaling involved in the development of cardiac hypertrophy (18, 26). The yeast strains used in this screen system lacked the pheromone receptor but expressed mammalian  $G\alpha$  ( $G\alpha_{13}$ ,  $G\alpha_s$ , or  $G\alpha_{16}$ ) in place of the yeast  $G\alpha$  subunit and provided a readout of growth upon activation of the G-protein-regulated pheromone signaling pathway. cDNA libraries from the left ventricle of the hypertrophy models were constructed in a galactose-inducible vector and introduced into these yeast strains. Functional screening for receptor-independent AGS proteins was then facilitated by selection of colonies growing in a galactose-specific manner.

We used two models of cardiac hypertrophy: the TAC-induced pressure overload model and the isoproterenol-induced tachycardiac hypertrophic model (supplemental Fig. 1). cDNA libraries from each model were introduced into the yeast strains expressing mammalian  $G\alpha_{13}$ ,  $G\alpha_s$ , or  $G\alpha_{16}$  (Table 1). Twenty-

## Transcriptional Regulation by Novel AGS

nine cDNA clones encoding six distinct proteins were isolated from the two cDNA libraries ( $G\alpha_s$  strain, 0;  $G\alpha_{i3}$  strain, 20;  $G\alpha_{16}$  strain, 9). Each clone was retransformed into yeast to confirm plasmid-dependent growth, and then epistasis analysis was performed to identify the site of action within the pheromone pathway. Epistasis analysis demonstrated that six of these cDNA clones required G-protein to activate the growth-linked

G-protein pathway, and thus these clones satisfied the definition of AGS (3, 27) (Table 1 and Fig. 1A).

Three clones isolated from yeast expressing  $G\alpha_{i3}$  encoded the previously characterized proteins AGS2 (*Dynlt1b*, NCBI Reference Sequence NM\_033368), AGS3 (*GPSM1*, NCBI Reference Sequence NM\_700459), and AGS6 (*RGS12*, NCBI Reference Sequence NM\_001156984). The cDNAs encoding AGS3 and AGS6 contained the G-protein-regulatory motif(s) that stabilizes the GDP-bound conformation of  $G\alpha_i$ , transducin, and  $G\alpha_o$ . An additional three cDNAs (1-8, 3-52, and 4-57) were isolated from yeast expressing  $G\alpha_{16}$ . These three cDNAs exhibited bioactivity in yeast strains expressing  $G\alpha_{16}$  but not in yeast expressing  $G\alpha_{i3}$ ,  $G\alpha_s$ , or  $G\alpha_1$  (yeast  $G\alpha$ ), indicating  $G\alpha$  selectivity (Fig. 1B and supplemental Text 1). We therefore focused on these  $G\alpha_{16}$ -specific AGS cDNAs.

**$G\alpha_{16}$ -specific AGS Proteins**—Sequence analysis of the  $G\alpha_{16}$ -specific cDNAs indicated that all encoded MITF/TFE transcription factors (31–33). cDNA1-8 encoded the C-terminal 533 amino acids of TFE3 (NCBI Reference Sequence NP\_766060), cDNA3-52 encoded the C-terminal 320 amino acids of TFE6 (NCBI Reference Sequence NP\_035679), and cDNA4-57 encoded the C-terminal 304 amino acids of MITF (NCBI Reference Sequence NP\_032627) (Fig. 1C). In accordance with the numbering of previously discovered AGS proteins (18), cDNA1-8, cDNA3-52, and cDNA4-57 were termed AGS11, AGS12, and AGS13, respectively (Table 1).

Full-length TFE3, TFE6, and MITF were cloned into a yeast expression vector, and the bioactivity for the G-protein signaling pathway was determined by  $\beta$ -galactosidase reporter assays (Fig. 1D). Full-length TFE3 and MITF, but not TFE6, activated the G-protein pathway in  $G\alpha_{16}$ -expressing cells. Full-length TFE3, MITF, and TFE6 did not activate growth of yeast expressing  $G\alpha_s$  (supplemental Text 2). Immunoblot analysis indicated that the full-length proteins were expressed at the

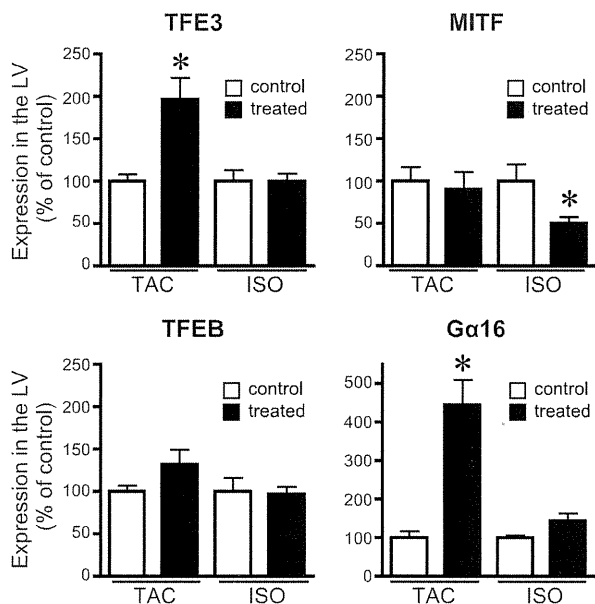


**FIGURE 2. Expression of MITF/TFE transcription factors and  $G\alpha_{16}$  in mouse cardiac hypertrophy model.** The expression of mRNA of each gene was analyzed by real time PCR as described under "Experimental Procedures." Control refers to the sham-operated or saline-infused mouse. Data are expressed as the -fold change in level compared with the control group. ISO, continuous infusion of isoproterenol; LV, left ventricle. Data are presented as the mean  $\pm$  S.E. of five experiments with duplicate determinations. \*,  $p < 0.05$  versus control group.

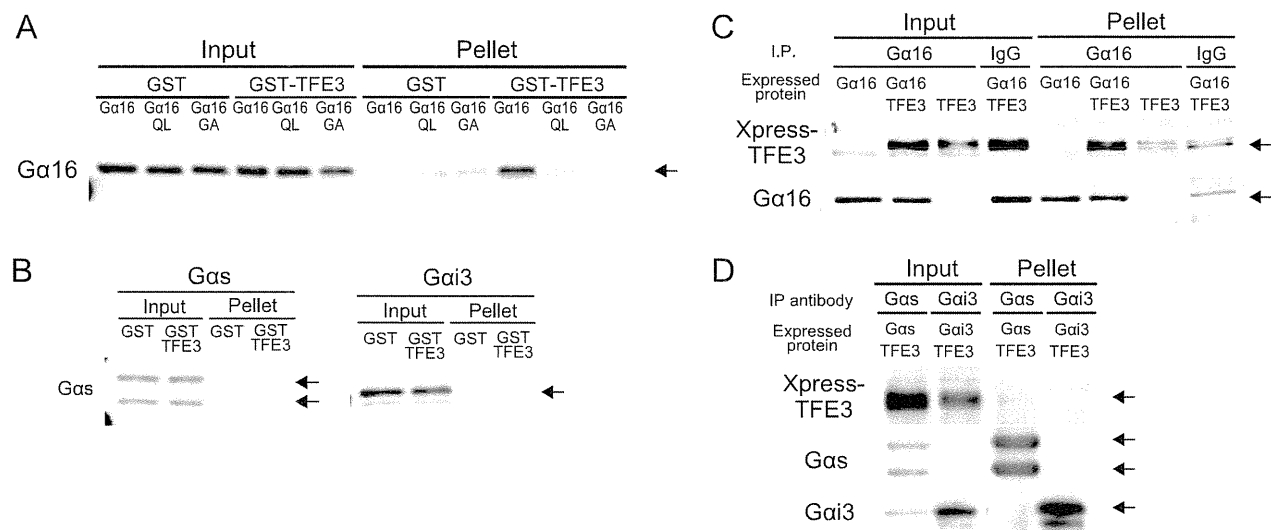


**FIGURE 3. Interaction of TFE3 with  $G\alpha_{16}$  in vitro and in cell.** A and B, GST pull-down assay of TFE3 with COS7 lysate expressing various  $G\alpha$  subunits. The C-terminal 533-amino acid fragment of TFE3 was expressed as a GST fusion protein (GST-TFE3). GST-TFE3 (300 nm) was incubated with 1 mg of cell lysate in a total volume of 500  $\mu$ l at 4  $^{\circ}$ C. Lysates of COS7 cells were prepared as described under "Experimental Procedures" following transfection of 10  $\mu$ g of the  $G\alpha$  subunit in pcDNA3. C and D, COS7 cells in a 100-mm dish were transfected with a combination of pcDNA3, pcDNA3:: $G\alpha_{16}$  (5  $\mu$ g/dish), and pcDNA3.1-His::TFE3 (5  $\mu$ g/dish). The amount of DNA transfected was adjusted to 10  $\mu$ g/well with the pcDNA3 vector. The preparation of a whole-cell lysate including the nuclear fraction and immunoprecipitation (IP) were performed as described under "Experimental Procedures." The  $G\alpha$  subunit was immunoprecipitated with a specific antibody for each  $G\alpha$  subunit. QL,  $G\alpha_{16}$ Q212L; GA,  $G\alpha_{16}$ G211A.

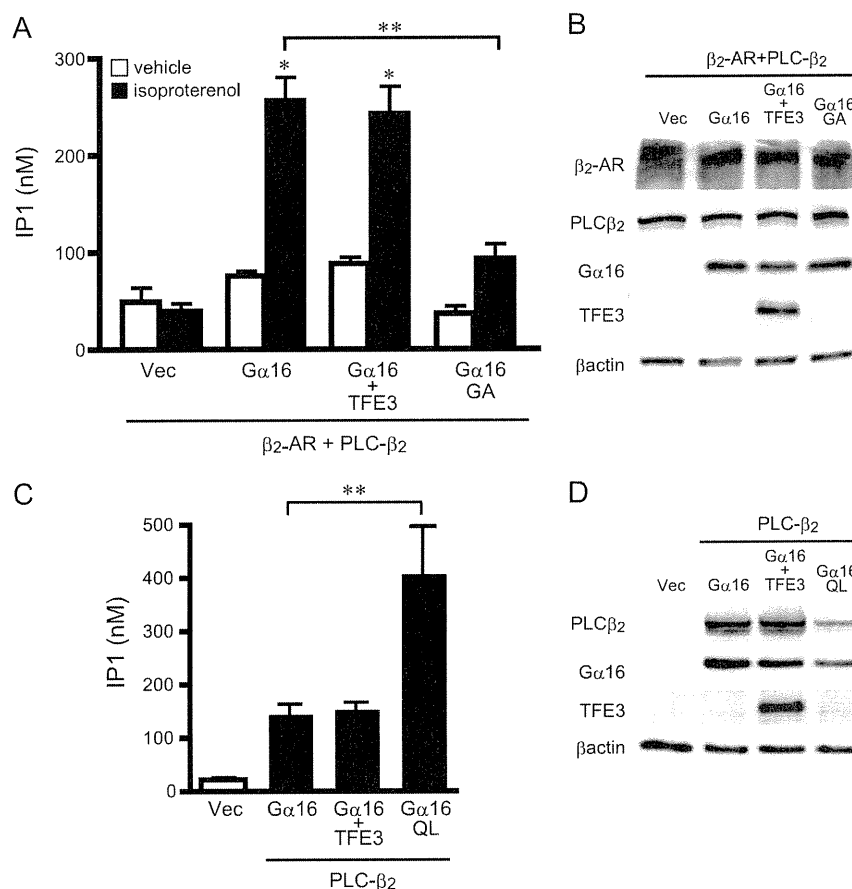


**FIGURE 4. Effect of TFE3 on activation of phospholipase C-β<sub>2</sub>.** *A*, effect of TFE3 on the generation of inositol phosphate (*IP*<sub>1</sub>) following receptor stimulation. COS7 cells were transfected in 12-well plates with control vectors (*Vec*) or cDNAs as indicated (0.4 μg of pcDNA::PLC-β<sub>2</sub>, 0.5 μg of pcDNA::TFE3, 0.5 μg of pcDNA::Gα<sub>16</sub>, and 0.6 μg of pEGFP::β<sub>2</sub>-adrenergic receptor (*AR*)). The amount of transfected DNA was adjusted to 2 μg/well with the pcDNA vector. Cells were stimulated with 10 μM isoproterenol for 30 min and assayed immediately. Data are expressed as the mean ± S.E. of five experiments with duplicate determinations. *B*, expression of transfected proteins of *A*. The expression of each protein was determined by immunoblotting of 10 μg of whole-cell lysates. *C*, effect of TFE3 on the generation of inositol phosphate. COS7 cells were transfected in 12-well plates with control vectors or cDNAs as indicated (0.5 μg of pcDNA::PLC-β<sub>2</sub>, 0.75 μg of pcDNA::TFE3, and 0.75 μg of pcDNA::Gα<sub>16</sub>). The amount of transfected DNA was adjusted to 2 μg/well with the pcDNA vector. Data are expressed as the mean ± S.E. of five experiments with duplicate determinations. *D*, expression of transfected cDNA of *C*. The expression of each protein was determined by immunoblotting of 10 μg of whole-cell lysates. \*, *p* < 0.05 versus control group; \*\*, *p* < 0.05 between two groups. QL, Gα<sub>16</sub>Q212L; GA, Gα<sub>16</sub>G211A.

expected size and that their expression did not alter the levels of Gα<sub>16</sub>. These findings suggest that TFE3, MITF, and TFEB are transcription factors that act as receptor-independent G-protein activators. AGSs with various functions have been identified; however, no transcription factors have previously been described as AGS proteins.

**Expression of TFE3, TFEB, and MITF in Cardiac Hypertrophy Models**—It was reported previously that the expression level of MITF was associated with development of cardiac hypertrophy in mouse (34). We sought to determine whether the three Gα<sub>16</sub>-specific AGS proteins were up-regulated in cardiac hypertrophy or were constitutively expressed in the myocardium. RNA expression of TFE3, MITF, TFEB, and the target Gα<sub>16</sub> subunit was determined in the hypertrophied myocardium (Fig. 2). TFE3 mRNA expression was up-regulated in the left ventricle in the TAC model but not in the isoproterenol model. MITF was unchanged in the TAC model but reduced in the isoproterenol model. TFEB did not show any significant changes of expression in either model. Notably, Gα<sub>16</sub> mRNA expression was also increased in the TAC model in which TFE3

was up-regulated. As TFE3 and Gα<sub>16</sub> were both significantly up-regulated in the TAC model, we focused on the characterization of TFE3.

**Formation of TFE3-Gα<sub>16</sub> Complex in Cells**—The above findings suggested that TFE3 plays an important role via Gα<sub>16</sub> in the development of cardiac hypertrophy. We thus examined whether TFE3 indeed was able to form a complex with Gα<sub>16</sub>. As a first approach, the interaction of GST-tagged TFE3 (GST-TFE3) with Gα<sub>16</sub> was examined *in vitro*. GST-TFE3 successfully pulled down transfected Gα<sub>16</sub> from cell lysates. However, neither a constitutively active mutant of Gα<sub>16</sub> (Gα<sub>16</sub>Q212L) nor an inactive mutant of Gα<sub>16</sub> (Gα<sub>16</sub>G211A) was pulled down, suggesting that the interaction of Gα<sub>16</sub> and TFE3 was dependent upon the conformation of Gα<sub>16</sub> and regulated by guanine nucleotide binding (Fig. 3A) (35, 36). In contrast, GST-TFE3 did not pull down transfected Gα<sub>s</sub> or Gα<sub>13</sub> from cell lysates (Fig. 3B). We also examined whether TFE3 interacted with Gα<sub>16</sub> in mammalian cells. Expressed TFE3 was co-immunoprecipitated with Gα<sub>16</sub> from COS7 cell lysates, suggesting that TFE3 and Gα<sub>16</sub> formed a stable complex

## Transcriptional Regulation by Novel AGS

within these cells (Fig. 3C). In contrast, TFE3 did not co-immunoprecipitate with  $G\alpha_s$  or  $G\alpha_{13}$  (Fig. 3D). We next examined the role of this interaction in  $G\alpha_{16}$ -mediated signaling events.

**TFE3 Is Not Involved in Receptor-mediated  $G\alpha_{16}$  Signaling—** $G\alpha_{16}$  is coupled to multiple GPCRs including  $\beta_2$ -adrenergic receptors mediating signal transfer to the effector molecule PLC- $\beta$  (37, 38). Thus, we examined whether TFE3 regulated  $\beta_2$ -adrenergic receptor-mediated PLC- $\beta$ 2 activation as a representative of  $G\alpha_{16}$ -mediated signaling (39). In a transient expression system in COS7 cells,  $G\alpha_{16}$  activated PLC- $\beta$ 2 following  $\beta_2$ -adrenergic receptor stimulation as determined by inositol monophosphate production (Fig. 4). The magnitude of PLC- $\beta$ 2 activation was reduced in the presence of an inactive  $G\alpha_{16}$  mutant ( $G\alpha_{16}G211A$ ), indicating that PLC- $\beta$ 2 activation was mediated by  $G\alpha_{16}$  (Fig. 4, A and B). However, TFE3 overexpression did not alter this receptor-mediated  $G\alpha_{16}$  signaling. We also examined the effect of TFE3 overexpression on the basal activity of PLC- $\beta$ 2/ $G\alpha_{16}$  in the absence of receptor stimulation. TFE3 overexpression did not alter PLC- $\beta$ 2 activity, whereas a constitutively active mutant of  $G\alpha_{16}$  ( $G\alpha_{16}Q212L$ ) increased the activity even in the absence of receptor stimulation (Fig. 4, C and D). These data are consistent with a lack of TFE3 involvement in regulating the conventional GPCR-mediated  $G\alpha_{16}$  signaling pathway.

**TFE3 Induces Accumulation of  $G\alpha_{16}$  in Nucleus—**The identification of transcription factors as  $G\alpha_{16}$ -specific AGS proteins suggested that MITF/TFE transcription factors may interact with a subpopulation of  $G\alpha_{16}$  distinct from that involved in the conventional G-protein signaling at the plasma membrane. To address this issue, we first examined the subcellular distribution of  $G\alpha_{16}$  and TFE3 when each was independently overexpressed in the cell. Overexpressed TFE3 was predominantly found in the nucleus as expected, whereas  $G\alpha_{16}$  was found in the plasma membrane and cytoplasm but not in the nucleus (Fig. 5, arrow, and supplemental Fig. 2, A, B, and D). However, when  $G\alpha_{16}$  and TFE3 were overexpressed together,  $G\alpha_{16}$  predominantly accumulated in the nucleus (Fig. 5, arrow). This novel nuclear translocation of  $G\alpha_{16}$  was not due to  $G\alpha_{16}$  activation because the constitutively active mutant of  $G\alpha_{16}$  ( $G\alpha_{16}Q212L$ ) was not found in the nucleus when it was overexpressed by itself. These data suggested that  $G\alpha_{16}$  forms a complex with TFE3 and translocates to the nucleus. Nuclear accumulation of G-protein by TFE3 was not observed for  $G\alpha_{13}$  or  $G\alpha_s$ .

**Up-regulation of Claudin 14 mRNA by TFE3- $G\alpha_{16}$  Complex—**The co-localization of TFE3 and  $G\alpha_{16}$  suggested an involvement of a nuclear TFE3- $G\alpha_{16}$  complex in regulating the expression of particular genes. To address this issue, genes regulated by TFE3 and  $G\alpha_{16}$  were screened by microarray analysis of mRNA of HEK293 cells transfected with TFE3 and/or  $G\alpha_{16}$ . In the screening of more than 40,000 human genes, we found that claudin 14 mRNA was highly up-regulated by the simultaneous transfection of TFE3 and  $G\alpha_{16}$ . Parallel experiments indicated that the co-overexpression of TFE3 and  $G\alpha_{16}$  in HEK293 cells increased claudin 14 mRNA by 133-fold, whereas independent overexpression of TFE3 (8.3-fold) or  $G\alpha_{16}$  (1.0-fold) had minimal effect on the induction of claudin 14 (Fig. 6A). The induc-

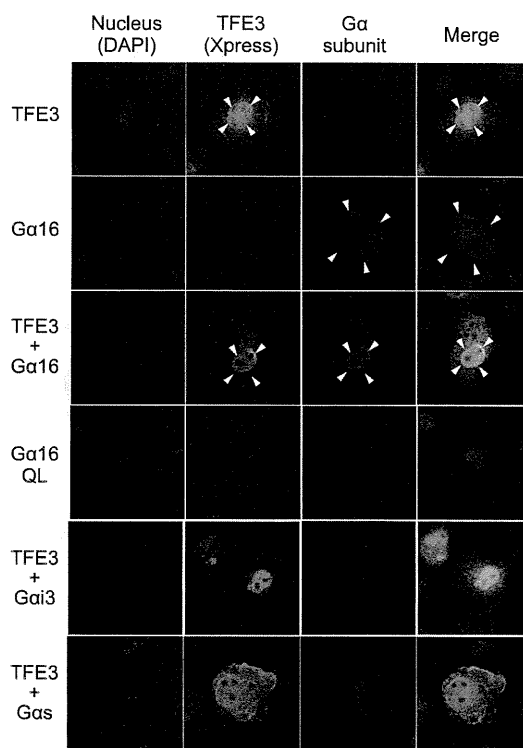


**FIGURE 5. Localization of expressed  $G\alpha$  subunits and TFE3 in COS7 cells.** COS7 cells were transfected in a 35-mm dish with 2.0  $\mu$ g of  $G\alpha$  subunits in pcDNA3 and/or 2.0  $\mu$ g of pcDNA3.1-His::TFE3. The amount of transfected DNA was adjusted to 4  $\mu$ g/well with the pcDNA3 vector. The  $G\alpha$  subunit and TFE3 were determined using a specific antibody for each  $G\alpha$  (red) or Xpress antibody (green), respectively. QL,  $G\alpha_{16}Q212L$ .

tion of claudin 14 was significantly decreased in the presence of the inactive mutant of  $G\alpha_{16}$  ( $G\alpha_{16}G211A$ ) compared with wild type  $G\alpha_{16}$ , suggesting that  $G\alpha_{16}$  activation was also required for the induction of this gene.

**Requirement of  $G\alpha_{16}$  Activation for Gene Induction by TFE3—**The requirement of  $G\alpha_{16}$  activation for this gene induction was further characterized utilizing a truncated mutant of TFE3 (delTFE3), which showed less bioactivity for  $G\alpha_{16}$  activation in the yeast system. Analysis of the amino acid sequences of the MITF/TFE family indicated that the C-terminal 27 acids were conserved among the  $G\alpha_{16}$ -selective AGS proteins (Fig. 6B, upper panel). Deletion of the C-terminal 27 amino acids resulted in the loss of bioactivity of TFE3 and MITF for G-protein activation (Fig. 6B, left middle panel, and supplemental Text 3). Despite the loss of bioactivity for  $G\alpha_{16}$  activation, delTFE3 was still able to form a complex with  $G\alpha_{16}$  and induce the translocation of  $G\alpha_{16}$  to the nucleus (Fig. 6B, left lower and right panels, and supplemental Fig. 2, C and D). Thus, nuclear translocation by itself did not require  $G\alpha_{16}$  activation as long as TFE3 and  $G\alpha_{16}$  formed a complex (Fig. 6A).

Although the delTFE3- $G\alpha_{16}$  complex was found in the nucleus, the subsequent up-regulation of claudin 14 was blunted, suggesting that  $G\alpha_{16}$  activation is critical for this gene induction (Fig. 6A). Furthermore, the constitutively active mutant of  $G\alpha_{16}$  ( $G\alpha_{16}Q212L$ ), which was not expressed in the nucleus (Fig. 5), failed to induce claudin 14. MITF, which had a similar ability to activate  $G\alpha_{16}$  (Fig. 1D), failed to induce claudin

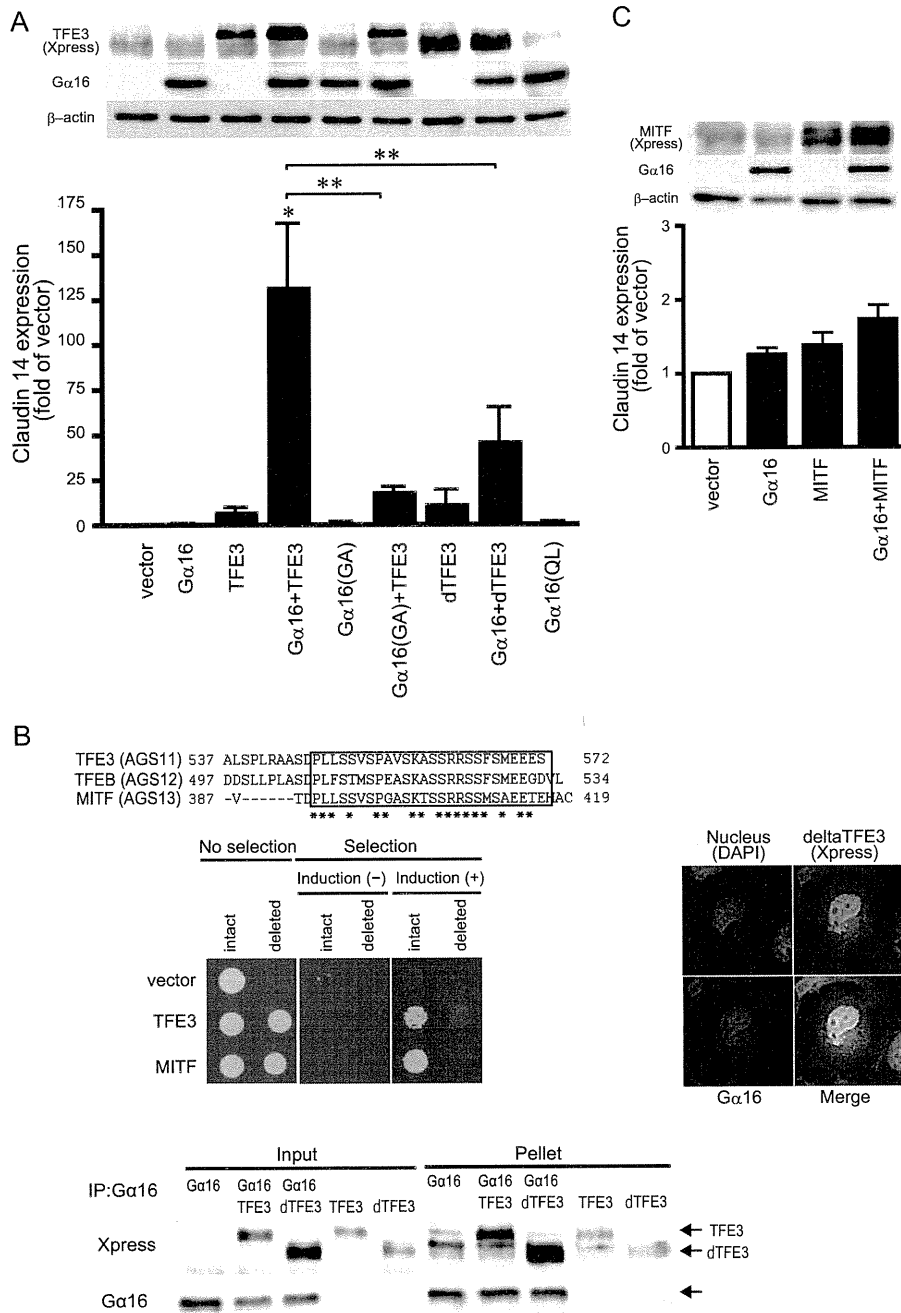


**FIGURE 6. Effect of TFE3 or MITF on expression of claudin 14.** *A*, expression of claudin 14 in transfected HEK293 cells. HEK293 cells were transfected in 6-well plates with a combination of control vectors or cDNAs as indicated (2.0  $\mu$ g of G $\alpha$  subunits in pcDNA3 and 2.0  $\mu$ g of TFE3 or delTFE3 in pcDNA3.1-His). The amount of transfected DNA was adjusted to 4  $\mu$ g/well with the pcDNA3 vector. The expression of claudin 14 mRNA was analyzed by real time PCR. Data are expressed as the -fold change from the level of claudin 14 expression in control cells transfected with the vector alone. Data are expressed as the mean  $\pm$  S.E. of five experiments with duplicate determinations. *Upper inset*, expression of proteins determined by immunoblotting ( $\sim$ 10  $\mu$ g of whole-cell lysate). Data are representative of five experiments. \*,  $p < 0.05$  versus control group; \*\*,  $p < 0.05$  between two groups. *B*, effect of delTFE3. *Upper panel*, amino acid sequence of C-terminal MITF/TFE transcription factors. The *square* indicates conserved amino acid sequence. \*, consensus amino acid. *Middle left panel*, bioactivity of intact or deleted TFE3 in yeast expressing G $\alpha$ <sub>16</sub>. The assay was performed as described under "Experimental Procedures." *Middle right panel*, localization of transfected G $\alpha$ <sub>16</sub> and TFE3 in COS7 cells. COS7 cells were transfected in a 35-mm dish with 2.0  $\mu$ g of pcDNA3::G $\alpha$ <sub>16</sub> and 2.0  $\mu$ g of pcDNA3.1-His::TFE3. G $\alpha$ <sub>16</sub> and TFE3 were determined using G $\alpha$ <sub>16</sub> antibody (red) or Xpress antibody (green), respectively. *Lower panel*, interaction of G $\alpha$ <sub>16</sub> with TFE3 or delTFE3. COS7 cells in a 100-mm dish were transfected with a combination of pcDNA3, pcDNA3::G $\alpha$ <sub>16</sub> (5  $\mu$ g/dish), pcDNA3.1-His::TFE3 (5  $\mu$ g/dish), and pcDNA3.1-His::delTFE3 (5  $\mu$ g/dish). The amount of transfected DNA was adjusted to 10  $\mu$ g/well with the pcDNA3 vector. The preparation of the cell lysate and immunoprecipitation (IP) were performed as described under "Experimental Procedures." *C*, effect of MITF on claudin 14 expression in transfected HEK293 cells. HEK293 cells were transfected in 6-well plates with a combination of control vectors or cDNAs as indicated (2.0  $\mu$ g of pcDNA3::G $\alpha$ <sub>16</sub> and 2.0  $\mu$ g of pcDNA3.1-His::MITF). The amount of transfected DNA was adjusted to 4  $\mu$ g/well with the pcDNA3 vector. The expression of claudin 14 mRNA was analyzed by real time PCR. Data are expressed as the -fold change in the level of claudin 14 in control cells transfected with the vector alone. Data are expressed as the mean  $\pm$  S.E. of five experiments with duplicate determinations. *Upper inset*, expression of proteins determined by immunoblotting ( $\sim$ 10  $\mu$ g of whole-cell lysate). Data are representative of five experiments. QL, G $\alpha$ <sub>16</sub>Q212L; GA, G $\alpha$ <sub>16</sub>G211A.

## Transcriptional Regulation by Novel AGS

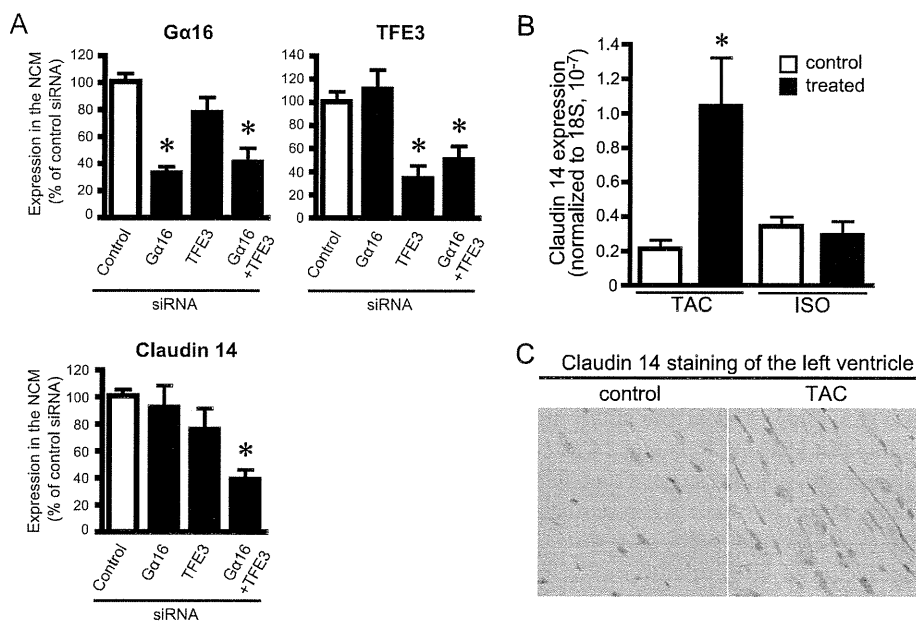


**FIGURE 7. Expression of claudin 14 in cultured cardiomyocytes and hypertrophied heart.** *A*, effect of knockdown of  $G\alpha_{16}$  and TFE3 on the level of claudin 14 mRNA in cultured cardiomyocytes. Neonatal cardiomyocytes (NCM) were transfected with each siRNA and/or universal control siRNA (Stealth RNAi Negative Control, Invitrogen). Forty-eight hours after transfection, the level of mRNA of  $G\alpha_{16}$  (*A*), TFE3 (*B*), and claudin 14 (*C*) were analyzed by real time PCR. Transfection efficiency of siRNA was estimated at 70–80% using FITC-labeled double strand RNA (Block It Fluorescent Oligo, Invitrogen) (right panel). \*,  $p < 0.05$  versus negative siRNA. Data are expressed as the mean  $\pm$  S.E. of seven to eight independent experiments. *B* and *C*, expression of claudin 14 in the mouse cardiac hypertrophy model. *B*, the left ventricular expression of claudin 14 mRNA was analyzed by real time PCR. Control refers to the sham-operated or saline-infused mouse. Data are expressed as the -fold change in claudin 14 level from that in control group. Data are expressed as the mean  $\pm$  S.E. of five experiments with duplicate determinations. *C*, immunohistochemical staining for claudin 14 (1:100; brown) of the left ventricle of sham- or TAC-operated mouse. A frozen section (8  $\mu$ m) of the mouse heart was subjected to immunohistochemical staining as described under "Experimental Procedures". Blue, nucleus. ISO, continuous infusion of isoproterenol. \*,  $p < 0.05$  versus control group.

14 (Fig. 6C). Taken together, the results suggest that in addition to the nuclear translocation of a TFE3- $G\alpha_{16}$  complex activation of  $G\alpha_{16}$  in the nucleus was required for the induction of claudin 14.

**Regulation of Claudin 14 Expression in Cardiomyocytes—**The influence of  $G\alpha_{16}$  and TFE3 on the expression of claudin 14 was also examined in neonatal cardiomyocytes following knockdown of  $G\alpha_{16}$  and/or TFE3 by siRNA.  $G\alpha_{16}$ siRNA or TFE3siRNA successfully suppressed the level of target molecules to 33–34% of the level of cardiomyocytes treated with negative control siRNA (Fig. 7A). The level of claudin 14 in cardiomyocytes was not influenced by  $G\alpha_{16}$ siRNA or TFE3siRNA itself when they were separately introduced (Fig. 7A, lower panel). However, interestingly, the simultaneous knockdown of  $G\alpha_{16}$  and TFE3 by siRNAs significantly reduced the claudin 14 mRNA ( $38.9 \pm 7.4\%$ ,  $p < 0.05$  versus control siRNA), indicating that both  $G\alpha_{16}$  and TFE3 were required for the regulation claudin 14 expression. These results are consistent with the data observed in HEK293 cells.

**Up-regulation of Claudin 14 in Mouse Heart upon Pressure Overload Stress—**As TFE3 and  $G\alpha_{16}$  were simultaneously up-regulated in the left ventricle in the TAC model (Fig. 2), we examined whether ventricular claudin 14 was also up-regulated in the models of cardiac hypertrophy. Quantitative PCR analysis indicated that claudin 14 mRNA was increased 5-fold in the left ventricle in the TAC model but not in the isoproterenol model of cardiac hypertrophy (Fig. 7B), consistent with the expression profile of TFE3 and  $G\alpha_{16}$  in these stimulated models (Fig. 2). Immunocytochemical analysis indicated that expres-

sion of claudin 14 was increased in the lateral membrane of cardiomyocytes rather than the intercalated disks (Fig. 7C). Thus, similar to our findings in cultured cells, the simultaneous up-regulation of TFE3 and  $G\alpha_{16}$  was associated with gene induction of claudin 14 *in vivo* under pathologic conditions. Gene induction by  $G\alpha_{16}$  and TFE3 is therefore postulated to be part of the cardiac adaptation process to pressure overload stress.

## DISCUSSION

We report the identification of three MITF/TFE transcription factors, TFE3, MITF, and TFEB, as new AGS proteins selective for the  $G\alpha_{16}$  subunit. These factors belong to the Myc supergene family of basic helix-loop-helix leucine zipper transcription factors that act either as a homo- or heterodimer within the family members (31–33). TFE3 formed a complex with and activated  $G\alpha_{16}$  in cells. Formation of TFE3- $G\alpha_{16}$  complex resulted in the translocation of  $G\alpha_{16}$  to the nucleus and up-regulation of the cell junction protein claudin 14. Expression of claudin 14 was also induced *in vivo* in the hypertrophied ventricle, and this was associated with the up-regulation of  $G\alpha_{16}$  and TFE3. Thus, the transcription factor TFE3 is postulated to act as a G-protein activator for the  $G\alpha_{16}$  subunit and regulate gene induction in response to pathophysiologic stress.

Although an increasing body of data implicates heterotrimeric G-proteins and their regulators as key regulators in multiple cellular events (40, 41), this is the first demonstration that activation of a  $G\alpha$  subunit by an AGS drives relocalization of  $G\alpha$  to the nucleus and gene transcription in mammalian cells.

Previous studies reported that heterotrimeric  $G\beta_5$  translocated to the nucleus when complexed with RGS7 (16). However, the effect of RGS7- $G\beta_5$  on gene regulation has not yet been characterized. This study is the first to demonstrate a direct effect of nuclear translocation of a  $G\alpha$  subunit on specific gene regulation.

The magnitude of gene induction by TFE3- $G\alpha_{16}$  was clearly dependent on the guanine nucleotide binding status of  $G\alpha_{16}$  as well as the bioactivity of TFE3 for  $G\alpha_{16}$  activation. Activation of  $G\alpha_{16}$  in the cytosol or plasma membrane was not sufficient to induce claudin 14 expression because a constitutively active  $G\alpha_{16}$  in the cytosol and plasma membrane failed to induce claudin 14 expression. Conversely, translocation of  $G\alpha_{16}$  to the nucleus by the delTFE3, which lacked the ability to activate  $G\alpha_{16}$ , showed a blunted induction of claudin 14 as compared with intact TFE3. These observations suggest that TFE3-mediated activation of  $G\alpha_{16}$  within the nucleus is essential to induce claudin 14 expression. TFE3 may serve as a direct guanine nucleotide exchange factor for  $G\alpha_{16}$  upon complex formation. Alternatively,  $G\alpha_{16}$  may be activated in the nucleus following removal or addition of a factor to the TFE3 complex when it is translocated into the nucleus.

The up-regulation of claudin 14 reported in this study may be an important event in remodeling of the heart following pressure overload stress. Claudin 14 was expressed in the lateral membrane of cardiomyocytes and was increased upon pressure overload stress. Claudin 14 is a member of the claudin family of more than 20 highly conserved proteins (42–44). It is interesting that the overexpression of claudin 14 induces apoptosis of cells independently of the caspase-mediated pathway (45). Moreover, in addition to its barrier function, claudin is also involved in activating pro-matrix metalloproteinase 2, which plays a role in reorganization of the extracellular matrix (46). Accordingly, the claudin-mediated sealing and/or molecular remodeling of the lateral region where cardiomyocytes are associated with the basal lamina or extracellular matrix is important for adaptation to mechanical stress. Indeed, changes in the expression of claudin 5 have been reported in the lateral membrane of cardiomyocytes in a dystrophic mouse with dilated cardiomyopathy (47, 48).

It is possible that the transcription factor MITF/TFE acts as a heterologous protein complex and binds to promoter regions to regulate the transcription of claudin 14. TFE3- $G\alpha_{16}$  may be required to assemble such a transcriptional complex, leading to increased transcription. Alternatively, TFE3- $G\alpha_{16}$  may regulate nuclear PLC- $\beta$  activity and the nuclear phosphoinositide cycle independently of the plasma membrane phosphoinositide cycle influencing cell cycle and cell differentiation (49). Activation of PLC- $\beta$  in the nucleus is not usually detectable in whole-cell experiments as used in this study (Fig. 4).

This is the first report of a regulatory protein for the  $G\alpha_{16}$  subunit, which can be coupled to multiple GPCRs in a variety of experimental systems (37, 38). Although  $G\alpha_{16}$  is enriched in hematopoietic tissue, it is also expressed in other tissues including heart (50, 51) where its expression is increased 4-fold by the cardiac stress induced in the TAC animal model. It is of particular interest to find that this multifunctional  $G\alpha_{16}$  is translo-

cated into the nucleus by a specific G-protein regulator where it plays a previously unappreciated functional role.

Various AGS proteins are involved in adaptation to various pathologic conditions (3, 20). For example, we previously identified AGS8 as a novel regulatory protein for the  $G\beta\gamma$  subunit in a repetitive transient ischemia model in the rat heart (18). AGS8 was up-regulated in the myocardium by ischemic/hypoxic stress and played a critical role in hypoxia-induced apoptosis of cardiomyocytes (18, 24). Our ability to rapidly identify AGS8 and now TFE3 directly from disease-specific mRNA libraries using our yeast-based functional screen highlights its usefulness in discovering disease-specific regulatory proteins for heterotrimeric G-proteins. Such disease-specific or adaptation-specific regulatory proteins represent novel therapeutic targets in treating human diseases.

*Acknowledgments*—We acknowledge Dr. James R. Broach (Molecular Biology, Princeton University, Princeton, NJ) and Cadus Pharmaceutical Corp. (New York, NY) for providing yeast strains used in this study. We thank Dr. Kazuhiro Ogata (Biochemistry and Gene Regulation, Yokohama City University) for helpful comments.

## REFERENCES

- Birnbaumer, L. (2007) *Biochim. Biophys. Acta* **1768**, 772–793
- Oldham, W. M., and Hamm, H. E. (2006) *Q. Rev. Biophys.* **39**, 117–166
- Sato, M., Blumer, J. B., Simon, V., and Lanier, S. M. (2006) *Annu. Rev. Pharmacol. Toxicol.* **46**, 151–187
- Cismowski, M. J. (2006) *Semin. Cell Dev. Biol.* **17**, 334–344
- Blumer, J. B., Smrcka, A. V., and Lanier, S. M. (2007) *Pharmacol. Ther.* **113**, 488–506
- Riddle, E. L., Schwartzman, R. A., Bond, M., and Insel, P. A. (2005) *Circ. Res.* **96**, 401–411
- Tall, G. G., and Gilman, A. G. (2005) *Proc. Natl. Acad. Sci. U.S.A.* **102**, 16584–16589
- Lee, M. J., and Dohlman, H. G. (2008) *Curr. Biol.* **18**, 211–215
- Garcia-Marcos, M., Ghosh, P., and Farquhar, M. G. (2009) *Proc. Natl. Acad. Sci. U.S.A.* **106**, 3178–3183
- Willars, G. B. (2006) *Semin. Cell Dev. Biol.* **17**, 363–376
- Du, Q., Stukenberg, P. T., and Macara, I. G. (2001) *Nat. Cell Biol.* **3**, 1069–1075
- Gotta, M., Dong, Y., Peterson, Y. K., Lanier, S. M., and Ahringer, J. (2003) *Curr. Biol.* **13**, 1029–1037
- Sanada, K., and Tsai, L. H. (2005) *Cell* **122**, 119–131
- Blumer, J. B., Kuriyama, R., Gettys, T. W., and Lanier, S. M. (2006) *Eur. J. Cell Biol.* **85**, 1233–1240
- Shu, F. J., Ramineni, S., Amyot, W., and Hepler, J. R. (2007) *Cell. Signal.* **19**, 163–176
- Hepler, J. R. (2005) *Sci. STKE* **2005**, pc38
- Sato, M., Gettys, T. W., and Lanier, S. M. (2004) *J. Biol. Chem.* **279**, 13375–13382
- Sato, M., Cismowski, M. J., Toyota, E., Smrcka, A. V., Lucchesi, P. A., Chilian, W. M., and Lanier, S. M. (2006) *Proc. Natl. Acad. Sci. U.S.A.* **103**, 797–802
- Blumer, J. B., Lord, K., Saunders, T. L., Pacchioni, A., Black, C., Lazar-tiques, E., Varner, K. J., Gettys, T. W., and Lanier, S. M. (2008) *Endocrinology* **149**, 3842–3849
- Sato, M., and Ishikawa, Y. (2010) *Pathophysiology* **17**, 89–99
- Hendriks-Balk, M. C., Peters, S. L., Michel, M. C., and Alewijnse, A. E. (2008) *Eur. J. Pharmacol.* **585**, 278–291
- Heximer, S. P., Srinivasa, S. P., Bernstein, L. S., Bernard, J. L., Linder, M. E., Hepler, J. R., and Blumer, K. J. (1999) *J. Biol. Chem.* **274**, 34253–34259
- Rogers, J. H., Tamirisa, P., Kovacs, A., Weinheimer, C., Courtois, M., Blumer, K. J., Kelly, D. P., and Muslin, A. J. (1999) *J. Clin. Investig.* **104**,

## Transcriptional Regulation by Novel AGS

- 567–576
24. Sato, M., Jiao, Q., Honda, T., Kurotani, R., Toyota, E., Okumura, S., Takaya, T., Minamisawa, S., Lanier, S. M., and Ishikawa, Y. (2009) *J. Biol. Chem.* **284**, 31431–31440
  25. Hill, J. A., Karimi, M., Kutschke, W., Davissou, R. L., Zimmerman, K., Wang, Z., Kerber, R. E., and Weiss, R. M. (2000) *Circulation* **101**, 2863–2869
  26. Cismowski, M. J., Takesono, A., Ma, C., Lizano, J. S., Xie, X., Fuernkranz, H., Lanier, S. M., and Duzic, E. (1999) *Nat. Biotechnol.* **17**, 878–883
  27. Takesono, A., Cismowski, M. J., Ribas, C., Bernard, M., Chung, P., Hazard, S., 3rd, Duzic, E., and Lanier, S. M. (1999) *J. Biol. Chem.* **274**, 33202–33205
  28. Cismowski, M. J., Takesono, A., Ma, C., Lanier, S. M., and Duzic, E. (2002) *Methods Enzymol.* **344**, 153–168
  29. Sato, M., Ribas, C., Hildebrandt, J. D., and Lanier, S. M. (1996) *J. Biol. Chem.* **271**, 30052–30060
  30. Sato, M., Kataoka, R., Dingus, J., Wilcox, M., Hildebrandt, J. D., and Lanier, S. M. (1995) *J. Biol. Chem.* **270**, 15269–15276
  31. Hodgkinson, C. A., Moore, K. J., Nakayama, A., Steingrímsson, E., Copeland, N. G., Jenkins, N. A., and Arnheiter, H. (1993) *Cell* **74**, 395–404
  32. Hughes, M. J., Lingrel, J. B., Krakowsky, J. M., and Anderson, K. P. (1993) *J. Biol. Chem.* **268**, 20687–20690
  33. Steingrímsson, E., Copeland, N. G., and Jenkins, N. A. (2004) *Annu. Rev. Genet.* **38**, 365–411
  34. Tshori, S., Gilon, D., Beeri, R., Nechushtan, H., Kaluzhny, D., Pikarsky, E., and Razin, E. (2006) *J. Clin. Investig.* **116**, 2673–2681
  35. Heasley, L. E., Storey, B., Fanger, G. R., Butterfield, L., Zamarripa, J., Blumberg, D., and Maue, R. A. (1996) *Mol. Cell. Biol.* **16**, 648–656
  36. Zhou, J., Stanners, J., Kabouridis, P., Han, H., and Tsoukas, C. D. (1998) *Eur. J. Immunol.* **28**, 1645–1655
  37. Huang, J., and Wilkie, T. M. (2006) *UCSD-Nature Molecule Pages* 10.1038/mp.a000972.01
  38. Offermanns, S., and Simon, M. I. (1995) *J. Biol. Chem.* **270**, 15175–15180
  39. Wu, D., Kuang, Y., Wu, Y., and Jiang, H. (1995) *J. Biol. Chem.* **270**, 16008–16010
  40. Burchett, S. A. (2003) *J. Neurochem.* **87**, 551–559
  41. Spiegelberg, B. D., and Hamm, H. E. (2007) *Curr. Opin. Genet. Dev.* **17**, 40–44
  42. Tsukita, S., and Furuse, M. (2002) *Curr. Opin. Cell Biol.* **14**, 531–536
  43. Wilcox, E. R., Burton, Q. L., Naz, S., Riazuddin, S., Smith, T. N., Ploplis, B., Belyantseva, I., Ben-Yosef, T., Liburd, N. A., Morell, R. J., Kachar, B., Wu, D. K., Griffith, A. J., Riazuddin, S., and Friedman, T. B. (2001) *Cell* **104**, 165–172
  44. Ben-Yosef, T., Belyantseva, I. A., Saunders, T. L., Hughes, E. D., Kawamoto, K., Van Itallie, C. M., Beyer, L. A., Halsey, K., Gardner, D. J., Wilcox, E. R., Rasmussen, J., Anderson, J. M., Dolan, D. F., Forge, A., Raphael, Y., Camper, S. A., and Friedman, T. B. (2003) *Hum. Mol. Genet.* **12**, 2049–2061
  45. Hu, Y., Lehrach, H., and Janitz, M. (2010) *Mol. Biol. Rep.* **37**, 3381–3387
  46. Miyamori, H., Takino, T., Kobayashi, Y., Tokai, H., Itoh, Y., Seiki, M., and Sato, H. (2001) *J. Biol. Chem.* **276**, 28204–28211
  47. Sanford, J. L., Edwards, J. D., Mays, T. A., Gong, B., Merriam, A. P., and Rafael-Fortney, J. A. (2005) *J. Mol. Cell. Cardiol.* **38**, 323–332
  48. Mays, T. A., Binkley, P. F., Lesinski, A., Doshi, A. A., Quaile, M. P., Margulies, K. B., Janssen, P. M., and Rafael-Fortney, J. A. (2008) *J. Mol. Cell. Cardiol.* **45**, 81–87
  49. Irvine, R. F. (2002) *Sci. STKE* **2002**, re13
  50. Wilkie, T. M., Scherle, P. A., Strathmann, M. P., Slepak, V. Z., and Simon, M. I. (1991) *Proc. Natl. Acad. Sci. U.S.A.* **88**, 10049–10053
  51. Giannone, F., Malpeli, G., Lisi, V., Grasso, S., Shukla, P., Ramarli, D., Sartoris, S., Monsurró, V., Krampera, M., Amato, E., Tridente, G., Colombatti, M., Parenti, M., and Innamorati, G. (2010) *J. Mol. Endocrinol.* **44**, 259–269





## Apoptosis in Heart Failure

### – The Role of the $\beta$ -Adrenergic Receptor-Mediated Signaling Pathway and p53-Mediated Signaling Pathway in the Apoptosis of Cardiomyocytes –

Takayuki Fujita, MD; Yoshihiro Ishikawa, MD

The heart works as a driving force to deliver oxygen and nutrients to the whole body. Interrupting this function for only several minutes can cause critical and permanent damage to the human body. Thus, heart failure (HF) or attenuated cardiac function is an important factor that affects both patient's the quality of life and longevity. Numerous clinical and basic studies have been performed to clarify the complex pathophysiology of HF and to develop effective therapies. Modulating the  $\beta$ -adrenergic receptor-mediated signaling pathway has been one of the most crucial targets for HF therapy. Impressively, recent reports identified p53, a well-known tumor suppressor, as a major player in the development of HF. The present review highlights the apoptosis of cardiomyocytes, which is one of the important mechanisms that leads to HF and can be induced by both  $\beta$ -adrenergic signaling and p53. Consideration of the cross-talk among these major pathways will be important when developing effective and safe therapies for HF. (*Circ J* 2011; 75: 1811–1818)

**Key Words:** Adrenergic signaling; Apoptosis; Heart failure; p53

**B**ecause the heart works as a driving force to deliver oxygen and nutrients to the whole body, cardiac function is a critical factor affecting quality of life and longevity. In addition, interrupting heart function for only a few minutes can cause critical and permanent damage to the human body. A report from the United States indicated that the lifetime risk of developing congestive heart failure (HF) is approximately 20%.<sup>1</sup> The most common cause of HF in Western countries is coronary artery disease (CAD). Although controlling the established risk factors for CAD has become more common in general healthcare and treating with several cardioprotective agents, including  $\beta$  blockers, RAS inhibitors, antiplatelet agents, and statins, improves the survival rate, the current prognosis for HF is still not acceptable. Therefore, further developments in HF treatment are one of the greatest issues for extending the healthy life of humans.

Numerous clinical and basic studies have been performed to clarify the complex pathophysiology of HF. These studies have identified several mechanisms that affect cardiac function, and some therapies were developed based on these results. Many years ago, the  $\beta$ -adrenergic receptor ( $\beta$ -AR)-mediated signaling pathway was identified as one of the most important pathways that regulates cardiac function. Modulating this pathway has been one of the most crucial targets for HF therapy.<sup>2</sup> On the other hand, recent reports identified p53, a well-known tumor suppressor, as a major player in the development of

HF.<sup>3–5</sup> The present review focuses on these 2 pathways.

Both pathways can induce the apoptosis of cardiomyocytes. It is well known that cardiomyocytes undergo apoptosis in response to harmful stimuli, including ischemia,<sup>6</sup> reperfusion,<sup>7</sup> oxidative stress,<sup>8</sup> stretching,<sup>9</sup> rapid pacing,<sup>10</sup> etc. Although some signaling mechanisms for inducing apoptosis in cardiomyocytes may be specific, such as those with Bim induction by EPAC,<sup>11</sup> others may be shared among different cell types. Since a 1997 report showed that failing hearts were associated with an increased number of apoptotic cardiomyocytes, the importance of apoptosis in the development of HF has been extensively examined and established in many reports.<sup>12</sup> The cell death of terminally differentiated cells, which cannot proliferate, directly affects tissue function. When attempting to develop an effective antiapoptotic therapy for the heart, we reviewed reports that examined the importance of each pathway in cardiomyocyte apoptosis. Based on these findings, we speculate that there is cross-talk among these pathways. Therefore, it will be important to take that into consideration when developing more effective and safe therapies.

#### $\beta$ -AR-Mediated Apoptosis of Cardiomyocytes

The positive inotropic effect of  $\beta$ -AR stimulation is one of the most effective measures for maintaining cardiac output during urgent care of HF. The  $\beta$ -AR stimulation induces protein kinase A (PKA) activation through G protein, adenylyl

Received January 24, 2011; revised manuscript received May 18, 2011; accepted May 30, 2011; released online July 11, 2011

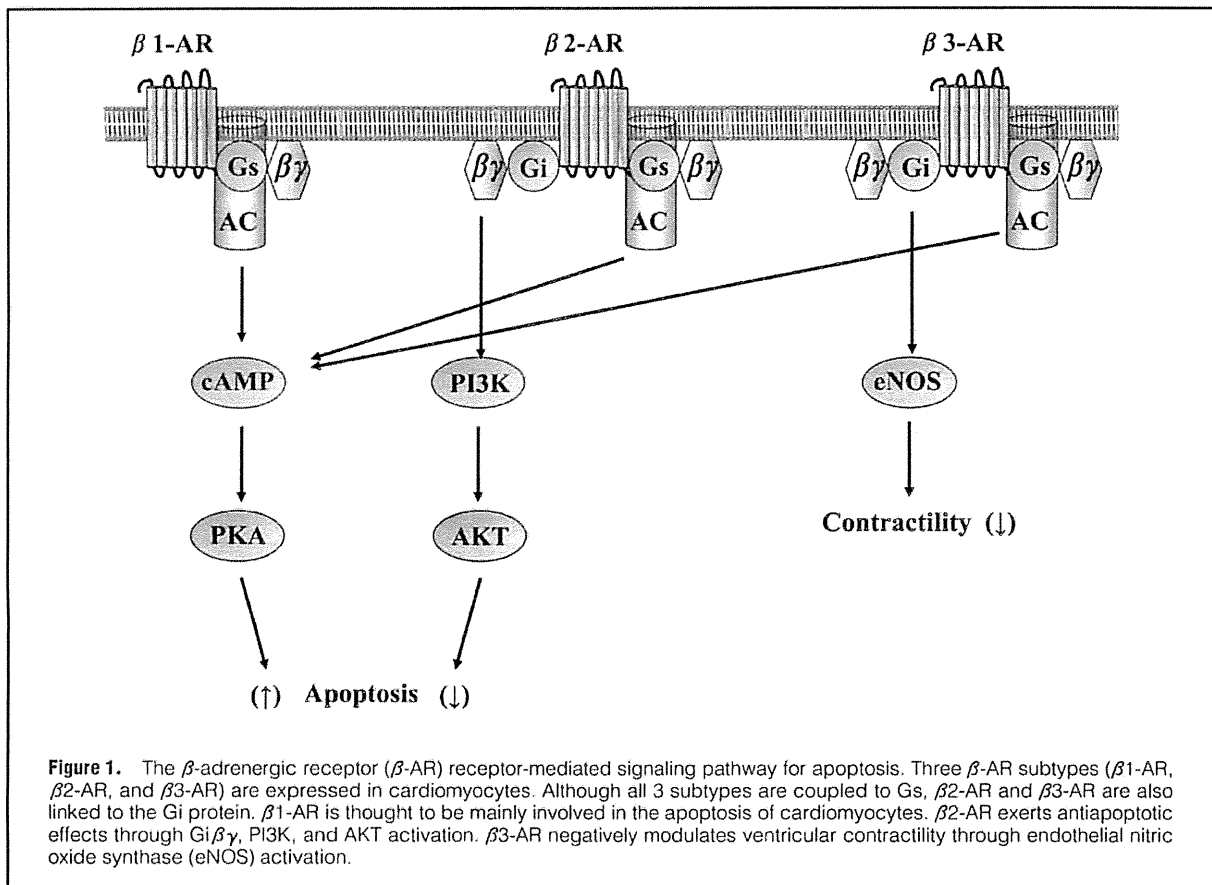
Cardiovascular Research Institute, Yokohama City University Graduate School of Medicine, Yokohama, Japan

Mailing address: Yoshihiro Ishikawa, MD, Cardiovascular Research Institute, Yokohama City University Graduate School of Medicine,

3-9 Fukuura, Kanazawa-ku, Yokohama 236-0004, Japan. E-mail: yishikaw@med.yokohama-cu.ac.jp

ISSN-1346-9843 doi:10.1253/circj.CJ-11-0025

All rights are reserved to the Japanese Circulation Society. For permissions, please e-mail: [cj@j-circ.or.jp](mailto:cj@j-circ.or.jp)



cyclase (AC) and cyclic adenosine monophosphate (cAMP).<sup>2</sup> PKA-mediated phosphorylation of many calcium-handling molecules enhances ventricular wall motion.<sup>13</sup> However, long-term stimulation of these receptors can lead to the deterioration of cardiac function. In addition, the prognosis of HF patients improves with  $\beta$ -AR blocking therapy.<sup>14</sup> One of the mechanisms that contributes to this phenomenon is thought to be the induction of apoptosis upon  $\beta$ -AR stimulation.<sup>15</sup> Failing hearts have been shown to have desensitized  $\beta$ -adrenergic receptor signaling. This response may help maintain cardiac function.<sup>16</sup>

Three  $\beta$ -AR subtypes ( $\beta$ 1-AR,  $\beta$ 2-AR, and  $\beta$ 3-AR) are expressed in cardiomyocytes (Figure 1). Norepinephrine or isoproterenol stimulates all  $\beta$ -AR subtypes and induces apoptosis in rat cardiomyocytes. However, not all subtypes of  $\beta$ -AR-mediated signaling induce cardiomyocyte apoptosis. It is thought that the  $\beta$ 1-AR-mediated pathway mainly contributes to apoptosis.<sup>17</sup> Although all 3 subtypes are coupled to Gs,  $\beta$ 2-AR and  $\beta$ 3-AR are also linked to the Gi protein. The  $\beta$ 2-AR exerts antiapoptotic effects through Gi $\beta\gamma$ , phosphatidylinositol-3 kinase (PI3K), and AKT activation.<sup>18</sup> In a rat model of myocardial infarction, treating with  $\beta$ 2-AR agonists for 2 weeks preserved cardiac contractility and reduced the number of apoptotic cardiomyocytes.<sup>19</sup> The  $\beta$ 3-AR expression is upregulated in the failing heart.<sup>20</sup> It is reported that  $\beta$ 3-AR negatively modulates ventricular contractility by activating endothelial nitric oxide synthase.<sup>21</sup> Although the role of  $\beta$ 3-AR-mediated signaling in cardiomyocyte apoptosis is

still unknown, it is possible that  $\beta$ 3-AR exerts antiapoptotic effects through nitric oxide.<sup>22</sup>

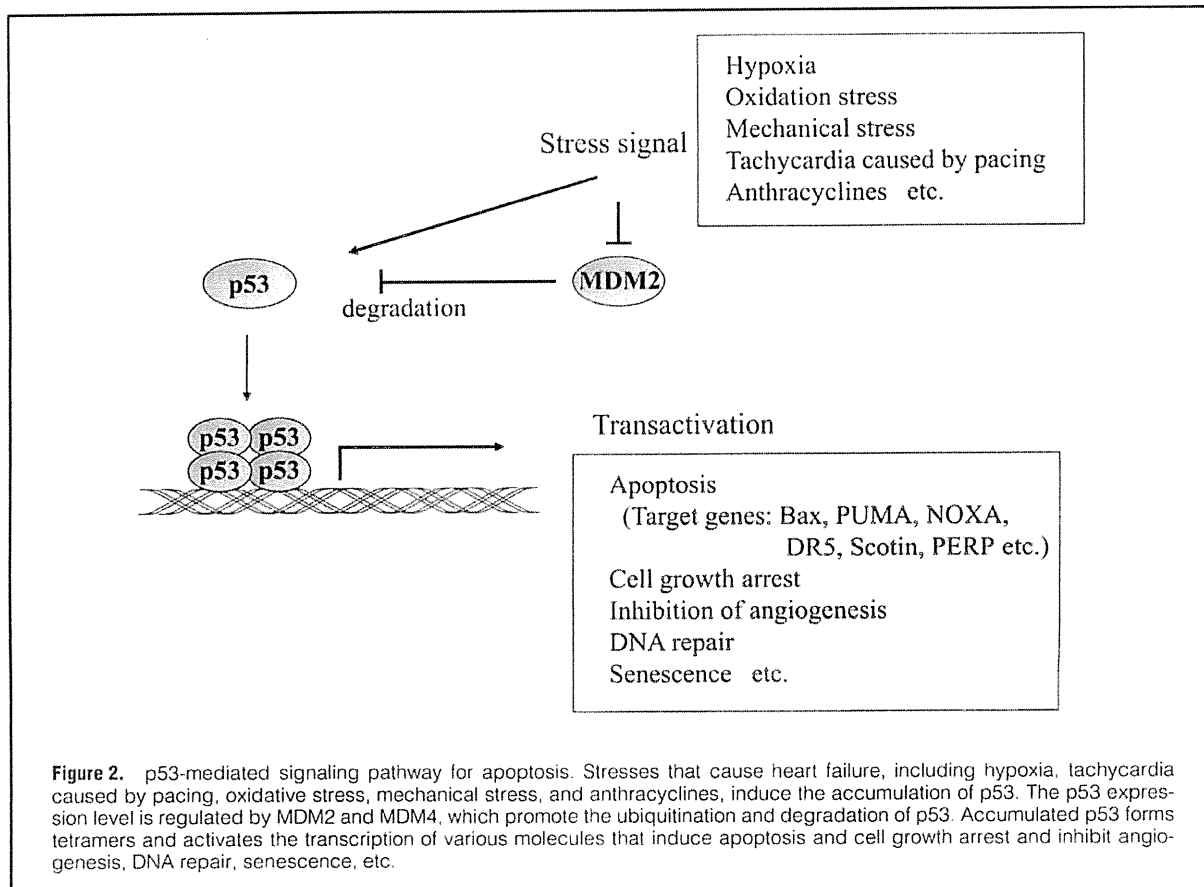
Several mechanisms of  $\beta$ -AR stimulation-induced apoptosis have been reported.

#### Inducible cAMP Early Repressor (ICER)

ICERs are a group of proteins that are produced from the cAMP responsive element modulator (CREM) gene and known to induce apoptosis. PKA, which is activated by  $\beta$ -AR stimulation, is a key molecule that maintains ICER expression. PKA activates the cAMP-responsive element binding protein (CREB), which transactivates ICER. In addition, PKA stabilizes ICER by reducing ubiquitination.<sup>23</sup> Moreover, ICER attenuates phosphodiesterase (PDE) 3A transcription by interacting with the promoter region of the PDE3A gene. The downregulation of PDE3A results in elevated cAMP levels. Consequently, cAMP–PKA–ICER–PDE forms a positive feedback loop that maintains ICER expression.

ICER promotes apoptosis by downregulating Bcl-2, which is an antiapoptotic protein. Consistent with this function, isoproterenol-treated cardiomyocytes were shown to have induced ICER expression, enhanced apoptosis, and decreased Bcl-2 expression.<sup>24</sup> In addition, similar results were obtained in cardiomyocytes that overexpressed ICER.

ICER includes a DNA-binding domain for a cAMP-responsive element (CRE), but lacks the CREM transactivation domain. Therefore, ICER inhibits CRE-mediated transcription by CREM/CREB. Inhibiting CRE-mediated transactiva-



tion of antiapoptotic signaling is thought to be another mechanism of ICER-induced apoptosis.

#### Ca<sup>2+</sup>/Calmodulin Kinase (CaMK), Calcineurin

$\beta$ -AR stimulation increases intracellular Ca<sup>2+</sup> through the L-type Ca<sup>2+</sup> channel, which is essential for the proapoptotic effects of  $\beta$ -adrenergic stimuli. The elevated intracellular Ca<sup>2+</sup> levels induce the activation of Ca<sup>2+</sup>-dependent kinase, CaMK, and the phosphatase, calcineurin. Both of these proteins reportedly mediate  $\beta$ -adrenergic signaling-induced apoptosis. The increase in the intracellular Ca<sup>2+</sup> concentration and CaMK activity is induced in a PKA-independent manner in cardiomyocytes.<sup>25</sup> However, the detailed mechanisms that lead to the proapoptotic effects of these proteins remain controversial. Calcineurin-independent induction of apoptosis was also observed in isoproterenol-treated cardiomyocytes.<sup>26,27</sup>

#### Exchange Protein Directly Activated by cAMP (EPAC)

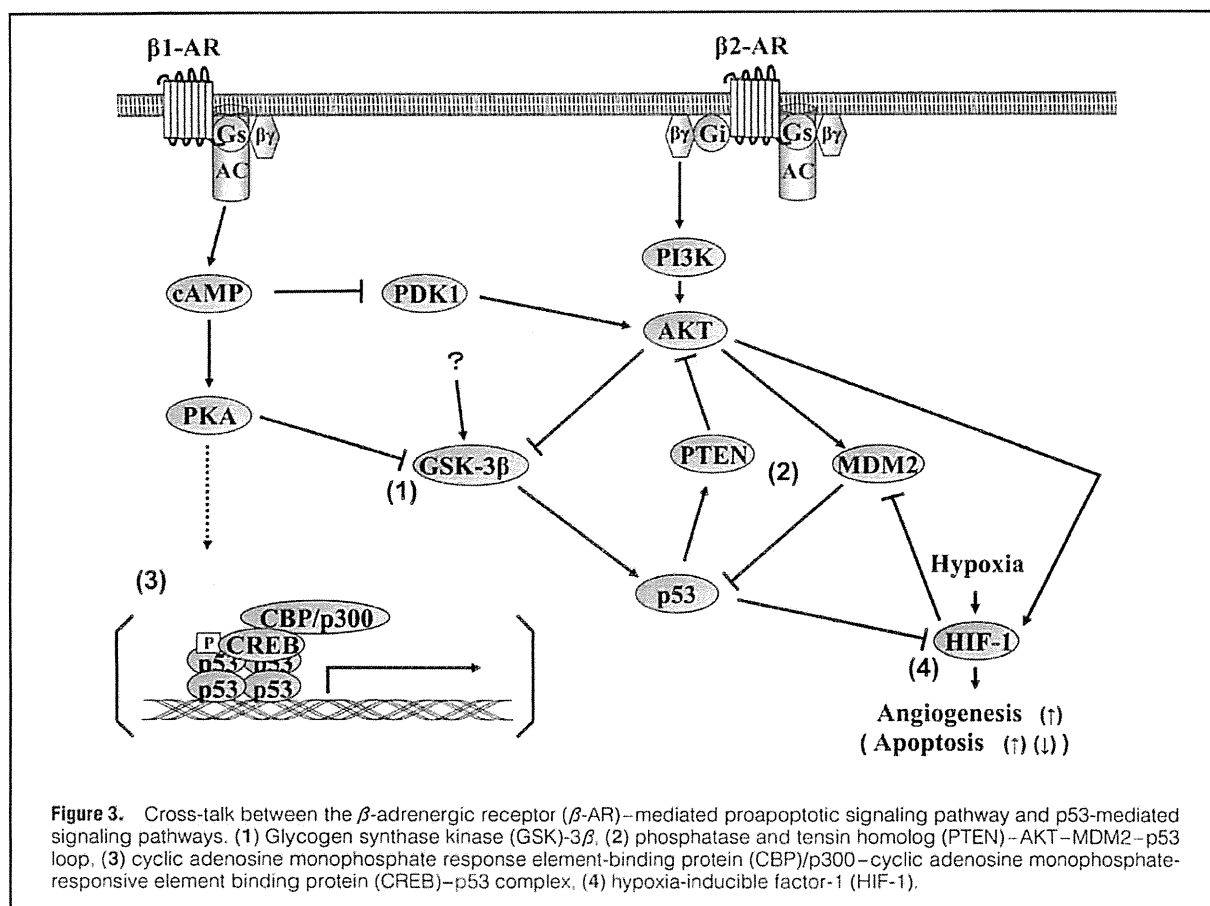
cAMP, which can be induced by  $\beta$ -AR stimulation, activates EPAC independently of PKA.<sup>28</sup> EPAC, a guanine nucleotide exchange factor for the Ras-like GTPase, is involved in several cellular processes, including cell differentiation, cell proliferation, cell survival, etc. EPAC was shown to exert proapoptotic effects by inducing Bim in neuronal cells.<sup>11</sup> Bim directly binds to the antiapoptotic protein Bcl-2, thereby inhibiting its function.<sup>29</sup> However, EPAC may not play a central role in cardiomyocyte apoptosis. Overexpressing EPAC in cardiomyocytes does not induce significant apoptosis and

1 reason for this finding may be that the heart does not express Bim.

#### p53-Mediated Apoptosis of Cardiomyocytes

p53 is one of the most famous proteins and a major tumor suppressor, which is a group of proteins that have been well studied in cancer research.<sup>30</sup> Mutations in the p53 gene that attenuate p53 function have been found in 50% of human cancers.<sup>31</sup> This finding indicates the importance of p53 in preventing cancer. p53 mainly functions as a transcription factor and induces a variety of molecules that induce apoptosis (Bax, p53 upregulated modulator of apoptosis (PUMA), NOXA, Death receptor 5 (DR5), Scotin, p53 apoptosis effector related to PMP-22 (PERP) etc.), arrest cell growth, inhibit angiogenesis, function in DNA repair, regulate senescence, etc (Figure 2). Accumulating evidence has elucidated the importance of p53 in various cellular responses. p53 is recognized as a key molecule in the adaptation to a wide variety of harmful stimuli, including hypoxia, oxidative stress, infection, etc. In the cardiovascular system, p53 was recently shown to have a crucial function in the development of HF, arteriosclerosis, cell senescence, metabolism, etc.

We review those reports on the relationship between p53 and HF with particular emphasis on the apoptosis of cardiomyocytes.



### p53 Expression During Stresses That Cause HF

A number of reports indicate that p53 expression is upregulated in the heart by the stresses that cause HF. Specifically, reports have shown that p53 is upregulated in the heart by ischemia,<sup>32,33</sup> oxidative stress,<sup>34</sup> mechanical stress,<sup>35</sup> and tachycardia caused by pacing.<sup>36</sup> Anthracyclines are anti-cancer agents that have been shown to cause cardiomyopathy, which leads to HF. Many reports demonstrated that treating with anthracyclines also induces p53 expression in cardiomyocytes.<sup>37</sup> In addition, involvement of telomere dysfunction induced p53 upregulation in the development of HF has been suggested.<sup>38,39</sup> Although not all reports support these findings,<sup>40</sup> accumulating evidence indicates that p53 plays an important role in stress-induced apoptosis in the heart.

### Roles of p53 in the Development of HF

Several studies have been conducted to clarify the roles of p53 in the development of HF. Many studies indicate that suppressing the function of p53 induces preferable effects on cardiac function. The function of p53 was attenuated by knocking out p53<sup>3</sup> or PUMA,<sup>41</sup> which mediates the proapoptotic effects of p53, and overexpressing MDM2,<sup>33</sup> which induces the ubiquitination and downregulation of p53. An examination of these models showed that these direct or indirect changes in p53 function resulted in decreased cardiomyocyte apoptosis, reduced myocardial infarct size, or a better survival rate after myocardial infarction. In addition, p53-deficient mice have decreased susceptibility to anthra-

cycline-induced myocardial apoptosis and HF.<sup>42</sup> On the other hand, knock-out mice for MDM4, which inhibits the accumulation of p53, develop cardiomyopathy.<sup>43</sup> In addition, overexpressing CHIP, which induces the degradation of p53, attenuated the accumulation of p53 and reduced cardiomyocyte apoptosis after myocardial infarction.<sup>4</sup> These findings indicate that p53 promotes the deterioration of cardiac function.

Recently, both apoptosis and inhibited angiogenesis were suggested to lead to the harmful effects of p53 on cardiac function. In a pressure overloaded mouse model, the cardiac condition transitions from an initial compensatory hypertrophy state to decompensatory HF several weeks after aortic banding. During this transition, p53 is upregulated, hypoxia-inducible factor-1 (HIF-1) expression is attenuated, and microvessels are reduced in the heart. HIF-1 is an established and major inducer of angiogenesis, and p53 was shown to play a pivotal role in downregulating HIF-1 expression during this transition.<sup>5,44</sup>

### Potential Crosstalk Between the $\beta$ -AR-Mediated Signaling Pathway and the p53-Mediated Signaling Pathway

Although there are only a few reports on the relationship between  $\beta$ -AR stimulation and the p53 expression level, p53 was shown to be upregulated in the presence of isoproterenol

in rat cultured cardiomyocytes.<sup>45</sup> In addition, p53 mRNA was also upregulated in cardiomyocytes that were isolated from a murine heart after long-term  $\beta$ -AR stimulation.<sup>46</sup>

On the other hand, p53 affects the expression level or activity of several molecules that can be involved in  $\beta$ -AR-mediated proapoptotic signal transduction, such as GSK-3 $\beta$  and HIF-1.

Accumulated findings obtained from studies of each pathway indicate that there are several possible cross-talk points between the  $\beta$ -AR- and p53-mediated signaling pathways during the induction of apoptosis (Figure 3).

#### Glycogen Synthase Kinase-3 $\beta$ (GSK-3 $\beta$ )

GSK-3 $\beta$  is a Ser/Thr protein kinase that phosphorylates and regulates many molecules that have a role in cell death, cell proliferation, cell growth, etc.<sup>47</sup> Several reports indicate that GSK-3 $\beta$  has proapoptotic effects in cardiomyocytes.<sup>48</sup> GSK-3 $\beta$  phosphorylates p53 and Bax, which facilitates proapoptotic signaling. In addition, 1 study reported that GSK-3 $\beta$  had a proapoptotic role in the isoproterenol-induced apoptosis of cultured adult rat cardiomyocytes.<sup>49</sup> These findings suggest that GSK-3 $\beta$  may have an important role in  $\beta$ -adrenergic signaling-induced p53 activation. On the other hand, GSK-3 $\beta$  can be inactivated via PKA- and AKT-mediated phosphorylation, which can be facilitated by the  $\beta$ -adrenergic signaling pathway.<sup>50</sup> Therefore, in contrast,  $\beta$ -AR stimulation can mediate antiapoptotic effects through GSK-3 $\beta$ . Although the mechanism by which  $\beta$ -AR stimulation induces apoptosis through the GSK-3 $\beta$  pathway is still unclear, studies suggest that a potent GSK-3 $\beta$ -activating pathway can overcome the effect on PKA- and AKT-mediated GSK-3 $\beta$  phosphorylation.

#### Phosphatase and Tensin Homolog (PTEN)-AKT-MDM2-p53 Loop

AKT (also known as protein kinase B) is involved in the development of hypertrophy, contractility, cell survival and inhibition of apoptosis in cardiomyocytes. The role of AKT in the heart was examined by developing a mouse model in which active AKT is specifically overexpressed in the heart. These mice had cardiac hypertrophy, increased contractility,<sup>51</sup> reduced infarct size and apoptosis after ischemia/reperfusion.<sup>52</sup> AKT is activated upon  $\beta$ -AR stimulation through PI3K and CaMK.<sup>50</sup> Therefore,  $\beta$ -AR stimuli-induced AKT activation may have a negative role in  $\beta$ -AR-induced apoptosis. Although  $\beta$ -AR signaling induces AKT activation through G $\beta$  $\gamma$ , at the same time Gs $\alpha$  that is also released from  $\beta$ -AR can inactivate AKT by inhibiting the membrane translocation of phosphoinositide-dependent protein kinase 1 (PDK1).<sup>53</sup> The expression levels of the molecules that are involved in these  $\beta$ -AR-induced pathways, including AC, are thought to be one of the deciding factors of the consequential effects on the role of these  $\beta$ -AR-induced pathways in AKT activity.<sup>54</sup>

AKT inhibits the accumulation of p53 by activating MDM2. When MDM2 is phosphorylated by AKT, MDM2 is translocated into the nucleus and promotes the degradation of p53. On the other hand, p53 inactivates AKT by transactivating PTEN. PTEN is a phosphatidylinositol phosphatase and a known antitumor molecule that inhibits AKT. PTEN overexpression causes apoptosis accompanied by AKT inactivation in cardiomyocytes.<sup>55</sup> Through this positive feedback loop (PTEN-AKT-MDM2-p53 loop),<sup>56</sup>  $\beta$ -AR-induced antiapoptotic signaling via AKT and p53-mediated proapoptotic signaling may eventually negatively affect each other. Regarding the  $\beta$ -AR-induced and p53-induced proapoptotic effects,

p53 promotes  $\beta$ -AR-induced apoptosis, while  $\beta$ -AR signaling may inhibit p53-induced apoptosis through the signaling loop.

#### Calcineurin and Nuclear Factor of Activated T Cell (NFAT)

NFAT is a transcription factor that induces a number of molecules that cause apoptosis, cardiac hypertrophy, cell cycle control, etc. NFAT is activated by the Ca<sup>2+</sup>/calmodulin-dependent phosphatase, calcineurin, which dephosphorylates NFAT, causing it to translocate from the cytoplasm to the nucleus. Carcinoma cells were shown to undergo p53-induced apoptosis through the calcineurin-dependent signaling pathway.<sup>57</sup> In addition, a previous report showed that both p53 and NFAT were involved in angiotensin II-induced apoptosis in vascular smooth muscle cells.<sup>57,58</sup> On the other hand, other reports have shown that calcineurin has a pivotal role in  $\beta$ -AR stimuli-induced apoptosis in cardiomyocytes.<sup>26</sup> Thus, calcineurin and NFAT may be involved in both the  $\beta$ -AR- and p53-mediated proapoptotic pathways.

#### Cyclic AMP Response Element-Binding Protein (CBP)/p300

CBP/p300 functions as a cofactor for several transcription factors, including p53, and facilitates their function. In addition, CBP/p300 was also shown to have histone acetyltransferase (HAT) activity. p53 is activated by CBP/p300 through acetylation.<sup>59</sup> When CBP/p300 activates p53, these 2 molecules form a tripartite complex with CREB. The formation of this complex is facilitated by the phosphorylation of CREB by PKA, CaMK, and protein kinase C.<sup>60,61</sup> PKA and CaMK are activated by  $\beta$ -AR signaling. Taken together, it can be speculated that there may be a situation in which  $\beta$ -adrenergic stimuli affect the p53 induced transactivation through the formation of the CBP/p300-CREB-p53 complex.

#### HIF-1

HIF-1 expression is induced by hypoxia and it predominantly functions as a transcription factor. HIF-1 transactivates a number of proteins that are involved in angiogenesis, cell proliferation, metabolism, cell survival, apoptosis, etc. HIF-1 can induce not only proapoptotic proteins such as BNIP3 and NIX, but also antiapoptotic proteins such as erythropoietin.<sup>62</sup> In addition, HIF-1 promotes the accumulation of p53 by directly interacting with MDM2.<sup>63</sup> Recent reports indicate that HIF-1 helps preserve cardiac function after hypoxic stress. HIF-1 overexpression attenuated cardiac damage after myocardial ischemia/reperfusion injury in cultured cardiomyocytes and a mouse model.<sup>64,65</sup> Although the enhancement of angiogenesis by HIF-1 is likely to be the important mechanism, several reports suggest that HIF-1 may modulate the apoptotic signal in cardiomyocytes.<sup>66-69</sup> Although the role of HIF-1 in the development of apoptosis is not well elucidated, HIF-1 is thought to be a potential factor in the apoptosis of cardiomyocytes.

HIF-1 expression is upregulated by the PI3K-AKT pathway,<sup>70</sup> which can be activated by G $\beta$  $\gamma$  protein-mediated signaling. In addition, Forskolin, an AC activator that can be activated by Gs protein, also induces HIF-1 expression in cancer cells.<sup>71</sup> On the other hand, some reports indicate that p53 downregulates HIF-1 expression. In addition, this downregulation is inhibited by AKT activation,<sup>72</sup> which can be induced by  $\beta$ -AR stimulation. Taken together,  $\beta$ -AR signaling upregulates, while p53 downregulates HIF-1 expression. Therefore, HIF-1-mediated regulation of apoptosis may be a type of competitive cross-talk between the  $\beta$ -AR- and p53-mediated signaling pathways.

However, only a few reports have examined this pathway in cardiomyocytes, so further studies are required in order to determine the importance of this pathway in the development of HF.

### Conclusions

It is crucial to maintain the number of cardiomyocytes in order to maintain the function of a failing heart. Although there have been several attempts to develop therapies that regenerate cardiomyocytes using stem cells or progenitor cells, currently there is not a clinically established method to increase in the number of cardiomyocytes.<sup>73,74</sup> Therefore, preventing cell death in the failing heart is still a promising approach to manage and prevent HF.

In this review, we focused on apoptosis as one mechanism of cell death in the failing heart. The  $\beta$ -AR- and p53-mediated signaling pathways are 2 major inducers of apoptosis. Many approaches, including gene therapy, have been developed to modulate the signaling of these pathways. Considering their effects on apoptosis, controlling these pathways could be a promising strategy to preserve cardiac function.

When attempting to establish HF therapies that modulate signal transduction, there are several important issues to be considered.

First, it is important to determine when and where signaling should be modulated. As the use of  $\beta$ -AR agonists or antagonists to treat HF depends on the disease state, the timing should be considered when modulating the p53 signaling pathways. p53 is a major tumor suppressor and may exacerbate HF by inducing apoptosis and inhibiting angiogenesis. However, p53 may also cause preferable effects on the heart. For example, p53 may inhibit the development of arteriosclerosis.<sup>75</sup> In addition, p53 may prevent the proliferation of vascular smooth muscle cells, which is pivotal in coronary restenosis after stent implantation.<sup>76</sup>

The  $\beta$ -antagonists have several side effects, including bronchial asthma, glucose intolerance, and Raynaud's phenomenon, because they affect tissues other than the heart. To avoid these effects, therapies that modulate specific subtypes of AC are near development.<sup>77</sup> In the same way, we should control p53 function in a tissue-specific manner.

Second, it is important to consider the possibility of cross-talk with other pathways that are involved in the development of HF. Modulating certain signaling pathways may affect others. Understanding the cross-talk among several important pathways would be useful in choosing the time and the method of therapeutic intervention to obtain the maximum effect. In this review, we noted 5 possible cross-talk points between the  $\beta$ -AR- and p53-mediated signaling pathways for apoptosis. Some of these are thought to facilitate another pathway. For example,  $\beta$ -adrenergic signaling may enhance the activity of p53 through several pathways. One of the mechanisms by which  $\beta$  blockers help preserve cardiac function may be by attenuating p53 function. On the other hand, potential points of competitive cross-talk have also been identified. For instance, p53 may downregulate HIF-1, while  $\beta$ -AR signaling may upregulate HIF-1. If there is a situation in which HIF-1 plays a significant role in regulating the apoptosis of cardiomyocytes, understanding these potentially interconnected pathways may lead to the development of more effective therapies that prevent apoptosis. Therefore, it will be important to examine the contribution of each pathway, as well as the cross-talk points under various conditions.

On the whole, to selectively inhibit the cAMP signaling

pathway while preserving the PI3K-AKT pathway seems to be effective for inhibiting the apoptosis that is induced by these 2 pathways. This fact reminds us of the  $\beta$ 1-selective  $\beta$  blockers. However, many pathways and molecules other than these 2 pathways are involved in the apoptosis of cardiomyocytes. Moreover, many mechanisms other than apoptosis are involved in the pathogenesis of HF. Cell death including necrosis, autophagy as well as  $Ca^{2+}$  handling, oxidative stress, metabolic state, etc have been identified as important factors that affect the development of HF. This may be one of the reasons why the advantages of  $\beta$ 1-selective  $\beta$  blockers compared with nonselective  $\beta$  blockers for HF therapy seem not to be significant in clinical studies. In the COMET trial, the  $\beta$ 1,  $\beta$ 2,  $\alpha$ 1 blocker, carvedilol, extended the longevity of chronic HF patients better than the  $\beta$ 1-selective blocker metoprolol.<sup>78</sup> Clarifying the relationships and roles of each signaling pathway in the various phases of HF development will lead to the development of more effective and sound treatments.

### References

- Lloyd-Jones DM, Larson MG, Leip EP, Beiser A, D'Agostino RB, Kannel WB, et al. Lifetime risk for developing congestive heart failure: The Framingham Heart Study. *Circulation* 2002; **106**: 3068–3072.
- Ishikawa Y, Homcy CJ. The adenylyl cyclases as integrators of transmembrane signal transduction. *Circ Res* 1997; **80**: 297–304.
- Matsusaka H, Ide T, Matsushima S, Ikeuchi M, Kubota T, Sunagawa K, et al. Targeted deletion of p53 prevents cardiac rupture after myocardial infarction in mice. *Cardiovasc Res* 2006; **70**: 457–465.
- Naito AT, Okada S, Minamino T, Iwanaga K, Liu ML, Sumida T, et al. Promotion of CHIP-mediated p53 degradation protects the heart from ischemic injury. *Circ Res* 2010; **106**: 1692–1702.
- Das B, Young D, Vasanthi A, Gupta S, Sarkar S, Sen S. Influence of p53 in the transition of myotrophin-induced cardiac hypertrophy to heart failure. *Cardiovasc Res* 2010; **87**: 524–534.
- Sato M, Jiao Q, Honda T, Kurotani R, Toyota E, Okumura S, et al. Activator of G protein signaling 8 (AGS8) is required for hypoxia-induced apoptosis of cardiomyocytes: Role of G betagamma and connexin 43 (CX43). *J Biol Chem* 2009; **284**: 31431–31440.
- Kang PM, Haunstetter A, Aoki H, Usheva A, Izumo S. Morphological and molecular characterization of adult cardiomyocyte apoptosis during hypoxia and reoxygenation. *Circ Res* 2000; **87**: 118–125.
- von Harsdorf R, Li PF, Dietz R. Signaling pathways in reactive oxygen species-induced cardiomyocyte apoptosis. *Circulation* 1999; **99**: 2934–2941.
- Liao X, Liu JM, Du L, Tang A, Shang Y, Wang SQ, et al. Nitric oxide signaling in stretch-induced apoptosis of neonatal rat cardiomyocytes. *FASEB J* 2006; **20**: 1883–1885.
- Kuramochi Y, Guo X, Sawyer DB, Lim CC. Rapid electrical stimulation induces early activation of kinase signal transduction pathways and apoptosis in adult rat ventricular myocytes. *Exp Physiol* 2006; **91**: 773–780.
- Suzuki S, Yokoyama U, Abe T, Kiyonari H, Yamashita N, Kato Y, et al. Differential roles of Epac in regulating cell death in neuronal and myocardial cells. *J Biol Chem* 2010; **285**: 24248–24259.
- Olivetti G, Abbi R, Quaini F, Kajstura J, Cheng W, Nitahara JA, et al. Apoptosis in the failing human heart. *N Engl J Med* 1997; **336**: 1131–1141.
- Yano M, Ikeda Y, Matsuzaki M. Altered intracellular  $Ca^{2+}$  handling in heart failure. *J Clin Invest* 2005; **115**: 556–564.
- Packer M, Bristow MR, Cohn JN, Colucci WS, Fowler MB, Gilbert EM, et al. The effect of carvedilol on morbidity and mortality in patients with chronic heart failure: U.S. Carvedilol Heart Failure Study Group. *N Engl J Med* 1996; **334**: 1349–1355.
- Communal C, Singh K, Pimentel DR, Colucci WS. Norepinephrine stimulates apoptosis in adult rat ventricular myocytes by activation of the beta-adrenergic pathway. *Circulation* 1998; **98**: 1329–1334.
- Bristow MR, Hershberger RE, Port JD, Gilbert EM, Sandoval A, Rasmussen R, et al. Beta-adrenergic pathways in nonfailing and failing human ventricular myocardium. *Circulation* 1990; **82**: 112–125.

17. Zaugg M, Xu W, Lucchinetti E, Shafiq SA, Jamali NZ, Siddiqui MA. Beta-adrenergic receptor subtypes differentially affect apoptosis in adult rat ventricular myocytes. *Circulation* 2000; **102**: 344–350.
18. Zhu WZ, Zheng M, Koch WJ, Lefkowitz RJ, Kobilka BK, Xiao RP. Dual modulation of cell survival and cell death by beta(2)-adrenergic signaling in adult mouse cardiac myocytes. *Proc Natl Acad Sci USA* 2001; **98**: 1607–1612.
19. Ahmet I, Krawczyk M, Heller P, Moon C, Lakatta EG, Talan MI. Beneficial effects of chronic pharmacological manipulation of beta-adrenoreceptor subtype signaling in rodent dilated ischemic cardiomyopathy. *Circulation* 2004; **110**: 1083–1090.
20. Moniotte S, Kobzik L, Feron O, Trochu JN, Gauthier C, Balligand JL. Upregulation of beta(3)-adrenoreceptors and altered contractile response to inotropic amines in human failing myocardium. *Circulation* 2001; **103**: 1649–1655.
21. Gauthier C, Leblais V, Kobzik L, Trochu JN, Khandoudi N, Bril A, et al. The negative inotropic effect of beta3-adrenoreceptor stimulation is mediated by activation of a nitric oxide synthase pathway in human ventricle. *J Clin Invest* 1998; **102**: 1377–1384.
22. Stefanelli C, Pignatti C, Tantini B, Stanic I, Bonavita F, Muscari C, et al. Nitric oxide can function as either a killer molecule or an anti-apoptotic effector in cardiomyocytes. *Biochim Biophys Acta* 1999; **1450**: 406–413.
23. Ding B, Abe J, Wei H, Xu H, Che W, Aizawa T, et al. A positive feedback loop of phosphodiesterase 3 (PDE3) and inducible cAMP early repressor (ICER) leads to cardiomyocyte apoptosis. *Proc Natl Acad Sci USA* 2005; **102**: 14771–14776.
24. Tomita H, Nazmy M, Kajimoto K, Yehia G, Molina CA, Sadoshima J. Inducible cAMP early repressor (ICER) is a negative-feedback regulator of cardiac hypertrophy and an important mediator of cardiac myocyte apoptosis in response to beta-adrenergic receptor stimulation. *Circ Res* 2003; **93**: 12–22.
25. Zhu WZ, Wang SQ, Chakir K, Yang D, Zhang T, Brown JH, et al. Linkage of beta1-adrenergic stimulation to apoptotic heart cell death through protein kinase A-independent activation of Ca<sup>2+</sup>/calmodulin kinase II. *J Clin Invest* 2003; **111**: 617–625.
26. Saito S, Hiroi Y, Zou Y, Aikawa R, Toko H, Shibasaki F, et al. Beta-Adrenergic pathway induces apoptosis through calcineurin activation in cardiac myocytes. *J Biol Chem* 2000; **275**: 34528–34533.
27. Grimm M, Brown JH. Beta-adrenergic receptor signaling in the heart: Role of CaMKII. *J Mol Cell Cardiol* 2010; **48**: 322–330.
28. Bos JL. Epac: A new cAMP target and new avenues in cAMP research. *Nat Rev Mol Cell Biol* 2003; **4**: 733–738.
29. O'Connor L, Strasser A, O'Reilly LA, Hausmann G, Adams JM, Cory S, et al. Bim: A novel member of the Bcl-2 family that promotes apoptosis. *EMBO J* 1998; **17**: 384–395.
30. Toledo F, Wahl GM. Regulating the p53 pathway: In vitro hypotheses, in vivo veritas. *Nat Rev Cancer* 2006; **6**: 909–923.
31. Vousden KH, Lu X. Live or let die: The cell's response to p53. *Nat Rev Cancer* 2002; **2**: 594–604.
32. Long X, Boluyt MO, Hipolito ML, Lundberg MS, Zheng JS, O'Neill L, et al. p53 and the hypoxia-induced apoptosis of cultured neonatal rat cardiac myocytes. *J Clin Invest* 1997; **99**: 2635–2643.
33. Toth A, Nickson P, Qin LL, Erhardt P. Differential regulation of cardiomyocyte survival and hypertrophy by MDM2, an E3 ubiquitin ligase. *J Biol Chem* 2006; **281**: 3679–3689.
34. Cesselli D, Jakoniuk I, Barlucchi L, Beltrami AP, Hintze TH, Nadal-Ginard B, et al. Oxidative stress-mediated cardiac cell death is a major determinant of ventricular dysfunction and failure in dog dilated cardiomyopathy. *Circ Res* 2001; **89**: 279–286.
35. Leri A, Claudio PP, Li Q, Wang X, Reiss K, Wang S, et al. Stretch-mediated release of angiotensin II induces myocyte apoptosis by activating p53 that enhances the local renin-angiotensin system and decreases the Bcl-2-to-Bax protein ratio in the cell. *J Clin Invest* 1998; **101**: 1326–1342.
36. Leri A, Liu Y, Malhotra A, Li Q, Stiegler P, Claudio PP, et al. Pacing-induced heart failure in dogs enhances the expression of p53 and p53-dependent genes in ventricular myocytes. *Circulation* 1998; **97**: 194–203.
37. Liu J, Mao W, Ding B, Liang CS. ERKs/p53 signal transduction pathway is involved in doxorubicin-induced apoptosis in H9c2 cells and cardiomyocytes. *Am J Physiol Heart Circ Physiol* 2008; **295**: H1956–H1965.
38. Oh H, Wang SC, Prahash A, Sano M, Moravec CS, Taffet GE, et al. Telomere attrition and Chk2 activation in human heart failure. *Proc Natl Acad Sci USA* 2003; **100**: 5378–5383.
39. Torella D, Rota M, Nurzynska D, Musso E, Monsen A, Shiraishi I, et al. Cardiac stem cell and myocyte aging, heart failure, and insulin-like growth factor-1 overexpression. *Circ Res* 2004; **94**: 514–524.
40. Webster KA, Discher DJ, Kaiser S, Hernandez O, Sato B, Bishopric NH. Hypoxia-activated apoptosis of cardiac myocytes requires reoxygenation or a pH shift and is independent of p53. *J Clin Invest* 1999; **104**: 239–252.
41. Toth A, Jeffers JR, Nickson P, Min JY, Morgan JP, Zambetti GP, et al. Targeted deletion of Puma attenuates cardiomyocyte death and improves cardiac function during ischemia-reperfusion. *Am J Physiol Heart Circ Physiol* 2006; **291**: H52–H60.
42. Shizukuda Y, Matoba S, Mian OY, Nguyen T, Hwang PM. Targeted disruption of p53 attenuates doxorubicin-induced cardiac toxicity in mice. *Mol Cell Biochem* 2005; **273**: 25–32.
43. Xiong S, Van Pelt CS, Elizondo-Fraire AC, Fernandez-Garcia B, Lozano G. Loss of Mdm4 results in p53-dependent dilated cardiomyopathy. *Circulation* 2007; **115**: 2925–2930.
44. Sano M, Minamoto T, Toko H, Miyauchi H, Orimo M, Qin Y, et al. p53-induced inhibition of Hif-1 causes cardiac dysfunction during pressure overload. *Nature* 2007; **446**: 444–448.
45. Zhou B, Wu LJ, Tashiro S, Onodera S, Uchiumi F, Ikejima T. Silibinin protects rat cardiac myocyte from isoproterenol-induced DNA damage independent on regulation of cell cycle. *Biol Pharm Bull* 2006; **29**: 1900–1905.
46. Kim KK, Soonpaa MH, Daud AI, Koh GY, Kim JS, Field LJ. Tumor suppressor gene expression during normal and pathologic myocardial growth. *J Biol Chem* 1994; **269**: 22607–22613.
47. Miura T, Miki T. GSK-3 $\beta$ , a therapeutic target for cardiomyocyte protection. *Circ J* 2009; **73**: 1184–1192.
48. Yin H, Chao L, Chao J. Kallikrein/kinin protects against myocardial apoptosis after ischemia/reperfusion via Akt-glycogen synthase kinase-3 and Akt-Bad.14-3-3 signaling pathways. *J Biol Chem* 2005; **280**: 8022–8030.
49. Menon B, Johnson JN, Ross RS, Singh M, Singh K. Glycogen synthase kinase-3 $\beta$  plays a pro-apoptotic role in beta-adrenergic receptor-stimulated apoptosis in adult rat ventricular myocytes: Role of beta1 integrins. *J Mol Cell Cardiol* 2007; **42**: 653–661.
50. Morisco C, Zebrowski D, Condorelli G, Tschlis P, Vatner SF, Sadoshima J. The Akt-glycogen synthase kinase 3 $\beta$  pathway regulates transcription of atrial natriuretic factor induced by beta-adrenergic receptor stimulation in cardiac myocytes. *J Biol Chem* 2000; **275**: 14466–14475.
51. Condorelli G, Drusco A, Stassi G, Bellacosa A, Roncarati R, Iaccarino G, et al. Akt induces enhanced myocardial contractility and cell size in vivo in transgenic mice. *Proc Natl Acad Sci USA* 2002; **99**: 12333–12338.
52. Fujio Y, Nguyen T, Wencker D, Kitsis RN, Walsh K. Akt promotes survival of cardiomyocytes in vitro and protects against ischemia-reperfusion injury in mouse heart. *Circulation* 2000; **101**: 660–667.
53. Kim S, Jee K, Kim D, Koh H, Chung J. Cyclic AMP inhibits Akt activity by blocking the membrane localization of PDK1. *J Biol Chem* 2001; **276**: 12864–12870.
54. Okumura S, Vatner DE, Kurotani R, Bai Y, Gao S, Yuan Z, et al. Disruption of type 5 adenylyl cyclase enhances desensitization of cyclic adenosine monophosphate signal and increases Akt signal with chronic catecholamine stress. *Circulation* 2007; **116**: 1776–1783.
55. Schwartzbauer G, Robbins J. The tumor suppressor gene PTEN can regulate cardiac hypertrophy and survival. *J Biol Chem* 2001; **276**: 35786–35793.
56. Oren M. Decision making by p53: Life, death and cancer. *Cell Death Differ* 2003; **10**: 431–442.
57. Rivero A, Maxwell SA. The p53-induced gene-6 (proline oxidase) mediates apoptosis through a calcineurin-dependent pathway. *J Biol Chem* 2005; **280**: 29346–29354.
58. Min LJ, Mogi M, Tamura K, Iwanami J, Sakata A, Fujita T, et al. Angiotensin II type 1 receptor-associated protein prevents vascular smooth muscle cell senescence via inactivation of calcineurin/nuclear factor of activated T cells pathway. *J Mol Cell Cardiol* 2009; **47**: 798–809.
59. Iyer NG, Ozdag H, Caldas C. p300/CBP and cancer. *Oncogene* 2004; **23**: 4225–4231.
60. Giebler HA, Lemasson I, Nyborg JK. p53 recruitment of CREB binding protein mediated through phosphorylated CREB: A novel pathway of tumor suppressor regulation. *Mol Cell Biol* 2000; **20**: 4849–4858.
61. Li B, Kaetzel MA, Dedman JR. Signaling pathways regulating murine cardiac CREB phosphorylation. *Biochem Biophys Res Commun* 2006; **350**: 179–184.
62. Sower HM, Ratcliffe PJ, Watson P, Greenberg AH, Harris AL. HIF-1-dependent regulation of hypoxic induction of the cell death factors BNIP3 and NIX in human tumors. *Cancer Res* 2001; **61**:

- 6669–6673.
63. Chen D, Li M, Luo J, Gu W. Direct interactions between HIF-1 alpha and Mdm2 modulate p53 function. *J Biol Chem* 2003; **278**: 13595–13598.
  64. Date T, Mochizuki S, Belanger AJ, Yamakawa M, Luo Z, Vincent KA, et al. Expression of constitutively stable hybrid hypoxia-inducible factor-1alpha protects cultured rat cardiomyocytes against simulated ischemia-reperfusion injury. *Am J Physiol Cell Physiol* 2005; **288**: C314–C320.
  65. Kido M, Du L, Sullivan CC, Li X, Deutsch R, Jamieson SW, et al. Hypoxia-inducible factor 1-alpha reduces infarction and attenuates progression of cardiac dysfunction after myocardial infarction in the mouse. *J Am Coll Cardiol* 2005; **46**: 2116–2124.
  66. Buhler K, Plaisance I, Dieterle T, Brink M. The human urocortin 2 gene is regulated by hypoxia: Identification of a hypoxia-responsive element in the 3'-flanking region. *Biochem J* 2009; **424**: 119–127.
  67. Kakinuma Y, Ando M, Kuwabara M, Katare RG, Okudela K, Kobayashi M, et al. Acetylcholine from vagal stimulation protects cardiomyocytes against ischemia and hypoxia involving additive non-hypoxic induction of HIF-1alpha. *FEBS Lett* 2005; **579**: 2111–2118.
  68. Recchia AG, De Francesco EM, Vivacqua A, Sisci D, Panno ML, Ando S, et al. The G protein-coupled receptor 30 is up-regulated by hypoxia-inducible factor-1{alpha} (HIF-1{alpha}) in breast cancer cells and cardiomyocytes. *J Biol Chem* 2010; **286**: 10773–10782.
  69. Malhotra R, Tyson DW, Rosevear HM, Brosius FC 3rd. Hypoxia-inducible factor-1alpha is a critical mediator of hypoxia induced apoptosis in cardiac H9c2 and kidney epithelial HK-2 cells. *BMC Cardiovasc Disord* 2008; **8**: 9.
  70. Jiang BH, Liu LZ. PI3K/P TEN signaling in angiogenesis and tumorigenesis. *Adv Cancer Res* 2009; **102**: 19–65.
  71. Park SY, Kang JH, Jeong KJ, Lee J, Han JW, Choi WS, et al. Norepinephrine induces VEGF expression and angiogenesis by a hypoxia-inducible factor-1alpha protein-dependent mechanism. *Int J Cancer* 2011; **128**: 2306–2316.
  72. Choy MK, Movassagh M, Bennett MR, Foo RS. PKB/Akt activation inhibits p53-mediated HIF1A degradation that is independent of MDM2. *J Cell Physiol* 2010; **222**: 635–639.
  73. Mignone JL, Kreutziger KL, Paige SL, Murry CE. Cardiogenesis from human embryonic stem cells. *Circ J* 2010; **74**: 2517–2526.
  74. Hosoda T, Kajstura J, Leri A, Anversa P. Mechanisms of myocardial regeneration. *Circ J* 2010; **74**: 13–17.
  75. Guevara NV, Kim HS, Antonova EI, Chan L. The absence of p53 accelerates atherosclerosis by increasing cell proliferation in vivo. *Nat Med* 1999; **5**: 335–339.
  76. Sata M, Tanaka K, Ishizaka N, Hirata Y, Nagai R. Absence of p53 leads to accelerated neointimal hyperplasia after vascular injury. *Arterioscler Thromb Vasc Biol* 2003; **23**: 1548–1552.
  77. Iwatsubo K, Minamisawa S, Tsunematsu T, Nakagome M, Toya Y, Tomlinson JE, et al. Direct inhibition of type 5 adenylyl cyclase prevents myocardial apoptosis without functional deterioration. *J Biol Chem* 2004; **279**: 40938–40945.
  78. Poole-Wilson PA, Swedberg K, Cleland JG, Di Lenarda A, Hanrath P, Komajda M, et al. Comparison of carvedilol and metoprolol on clinical outcomes in patients with chronic heart failure in the Carvedilol Or Metoprolol European Trial (COMET): Randomised controlled trial. *Lancet* 2003; **362**: 7–13.



Full Paper

## Electrophysiological and Pharmacological Characteristics of Triggered Activity Elicited in Guinea-Pig Pulmonary Vein Myocardium

Akira Takahara<sup>1,\*</sup>, Takahiko Sugimoto<sup>1</sup>, Takuma Kitamura<sup>1</sup>, Kiyoshi Takeda<sup>1</sup>, Yayoi Tsuneoka<sup>1</sup>, Iyuki Namekata<sup>1</sup>, and Hikaru Tanaka<sup>1</sup>

<sup>1</sup>Department of Pharmacology, Toho University Faculty of Pharmaceutical Sciences, Funabashi, Chiba 274-8510, Japan

Received September 10, 2010; Accepted December 5, 2010

**Abstract.** The pulmonary vein is known as an important source of ectopic beats, initiating frequent paroxysms of atrial fibrillation. We analyzed electrophysiological and pharmacological characteristics of triggered activity elicited in the isolated pulmonary vein from the guinea pig. Immediately after the termination of train stimulation (pacing cycle length of 100 ms), spontaneous activities accompanied with phase-4 depolarization were detected in 43 out of 45 pulmonary vein preparations. Such triggered activities were not observed in the isolated left atrium. The incidence of triggered activity was higher at a shorter pacing cycle length (100 – 200 ms), and the coupling interval was shorter at a shorter pacing cycle length. Verapamil (1  $\mu$ M), ryanodine (0.1  $\mu$ M), and pilsicainide (10  $\mu$ M) suppressed the occurrence of triggered activities. The resting membrane potential of the pulmonary vein myocardium was more positive than that of the left atrium. Carbachol (0.3  $\mu$ M) hyperpolarized the resting membrane potential and completely inhibited the occurrence of triggered activities. These results suggest that the pulmonary veins have more arrhythmogenic features than the left atrium, possibly through lower resting membrane potential. The electrophysiological and pharmacological characteristics of triggered activity elicited in the pulmonary vein myocardium were similar to those previously reported using ventricular tissues.

**Keywords:** triggered activity, pulmonary vein, left atrium, membrane potential, carbachol

### Introduction

Atrial fibrillation is known as the most common cardiac arrhythmia in adults, which is a major cause of stroke (1). Whereas the arrhythmia has been recognized to be perpetuated by reentrant wavelets propagating in an abnormal atrial-tissue substrate, Haïssaguerre et al. found in 1998 that the origin of atrial ectopic beats was localized in the pulmonary vein myocardial sleeve of patients with drug-resistant atrial fibrillation (2). Cheung reported in 1980 that isolated pulmonary vein preparations from guinea pigs were capable of independent pace-making activity (3). Recently, electrophysiological characteristics of the pulmonary vein have been extensively analyzed in isolated rabbit or dog preparations, which show that the combination of reentrant and non-reentrant mechanisms is the underlying arrhythmogenic mechanisms of atrial

fibrillation from the pulmonary veins (4 – 6).

Triggered activity is one of the well-recognized mechanisms of ectopy aggravated by an increased rate of beating (7 – 9). Tactics to raise the intracellular  $Ca^{2+}$  concentration of the ventricular tissues, such as treatment with digitalis or a low  $K^+$  / high  $Ca^{2+}$  extracellular environment, causes an oscillatory  $Ca^{2+}$  release from the sarcoplasmic reticulum and transient depolarization after completion of ventricular repolarization (10). The delayed afterdepolarization (DAD) and resulting triggered activity have been shown to be effectively suppressed by  $Na^+$ -channel blockers,  $Ca^{2+}$ -channel blockers, and ryanodine in isolated ventricular preparations (11, 12). DAD-related triggered activity has been demonstrated in isolated pulmonary vein myocardium or its isolated cardiomyocytes (13, 14). However, fundamental electrophysiological characteristics of triggered activity have never been examined, such as the relationship between pacing rate to induce triggered activity and its incidence or coupling interval (10). In this study, to better understand the arrhythmogenic activity of the pulmonary vein

\*Corresponding author. akirat@phar.toho-u.ac.jp  
Published online in J-STAGE on January 18, 2011 (in advance)  
doi: 10.1254/jphs.10232FP

itself, we analyzed electrophysiological and pharmacological characteristics of the triggered activity in isolated guinea-pig pulmonary vein. Triggered activity was induced by train stimulation, which is known as a useful methodology to reproducibly induce DAD-related triggered activity (10, 12, 15).

### Materials and Methods

All experiments were approved by the Ethics Committee of Toho University Faculty of Pharmaceutical Sciences and performed in accordance with the Guiding Principles for the Care and Use of Laboratory Animals approved by The Japanese Pharmacological Society. The heart and adjunct lungs were isolated from male or female Hartley guinea pigs weighing 350–450 g. The pulmonary veins were separated from the left atrium and lung at the end of the pulmonary vein myocardium sleeve in Krebs-Henseleit solution of the following composition: 118.4 mM NaCl, 4.7 mM KCl, 2.5 mM CaCl<sub>2</sub>, 1.2 mM MgSO<sub>4</sub>, 1.2 mM KH<sub>2</sub>PO<sub>4</sub>, 24.9 mM NaHCO<sub>3</sub>, and 11.1 mM glucose, gassed with 95% O<sub>2</sub> / 5% CO<sub>2</sub> (pH 7.4 at 37°C).

### Histological examinations

Pulmonary veins were fixed with 10% formalin neutral buffer solution, and the segments were processed into paraffin blocks. The paraffinized tissue blocks were cut into 4- $\mu$ m-thick sections and mounted on charged slides. For each paraffin block, one slide each was stained with Masson trichrome to accentuate muscle and connective tissues. A serial section was incubated with antibodies against  $\alpha$ -smooth muscle actin ( $\alpha$ -SMA, 1:500; Dako, Glostrup, Denmark) followed by consecutive incubations with universal immuno-peroxydase polymer (Histofine<sup>®</sup>, Simple Stain Rat MAX PO MULTI; Nichirei Bioscience, Tokyo). Antibody binding was demonstrated by staining with 3,3'-diaminobenzidine tetrahydrochloride.

### Microelectrode recording of action potential configuration

The luminal side of the pulmonary vein at the middle region between the ostium and the distal end of myocardial sleeve or endocardial surface of the left atrium was impaled with glass microelectrodes filled with 3 M KCl to record transmembrane potential using a microelectrode amplifier (Intra 767; World Precision Instruments, Sarasota, FL, USA). The action potential signals were monitored by an oscilloscope (CS-5135; Kenwood, Tokyo) and fed into a waveform analysis system (DSS98-type IV, from Canopus, Tokyo or PowerLab, from ADInstruments, Castle Hill, Australia). All experiments were performed at 36.5  $\pm$  0.5°C.

Triggered activity was induced by a burst pacing of 100 train pulses at a pacing cycle length of 100, 150, or 200 ms using an electronic stimulator (SEN-2201; Nihon Kohden, Tokyo) with rectangular current pulses (3-ms duration, about 1.5 threshold) through bipolar platinum electrodes. Action potential parameters, including resting potential (RP), overshoot (OS), and action potential duration at 20% (APD<sub>20</sub>), 50% (APD<sub>50</sub>), and 90% (APD<sub>90</sub>) repolarization, were measured under electrical stimulation at a constant frequency of 1 Hz. The action potentials of the pulmonary vein were of the fast-response type, and neither early afterdepolarizations (EADs) nor DADs were observed in the preparations electrically driven at 1 Hz.

### Drugs

Verapamil hydrochloride and carbachol were purchased from Sigma-Aldrich (St. Louis, MO, USA), and ryanodine was obtained from Wako (Osaka). Pilsicainide hydrochloride was kindly provided by Daiichi-Sankyo Co., Ltd. (Tokyo). Ryanodine was initially dissolved in dimethylsulfoxide and diluted to 0.01% dimethylsulfoxide in the Krebs-Henseleit solution. Other drugs were dissolved in distilled water and small aliquots were added to the organ bath to obtain the desired final concentration. All other chemicals were commercial products of the highest available quality.

### Statistical analyses

Statistical significance between means was evaluated by the one-way repeated measures analysis of variance followed by Contrasts for mean values comparison or by Dunnett's test. A *P*-value less than 0.05 was considered significant.

### Results

#### Histology of the pulmonary vein

Typical photomicrographs of longitudinal sections of the left superior pulmonary vein obtained from the guinea pig are shown in Fig. 1. Vascular smooth muscle was detected on the luminal face of the pulmonary vein, whereas a myocardial sleeve was observed at mid-layer of the pulmonary vein.

#### Triggered activities in the pulmonary vein

Figure 2A shows a typical tracing of burst pacing-induced triggered activity in the pulmonary vein preparation. After the train stimulation at a pacing cycle length of 100 ms, spontaneous activities accompanied with phase-4 depolarization were detected in 43 out of 45 pulmonary vein preparations. On the other hand, phase-4 depolarization was not detected in the left atrium prepa-

rations examined ( $n = 8$ ). As shown in the Table 1, the incidence of triggered activity and number of premature beats were greater after the faster train stimulation. The coupling interval decreased in a frequency-dependent manner.

#### Effects of pharmacological intervention on the triggered activity

At the pre-drug period, the number of triggered activity, which was induced after the 100-train stimulation at a pacing cycle length of 100 ms, was  $2.4 \pm 0.2$  in the control group,  $2.6 \pm 0.9$  in the pilsicainide group,  $2.4 \pm 0.7$  in the ryanodine group, and  $2.4 \pm 0.4$  in the verapamil group. There were no significant differences

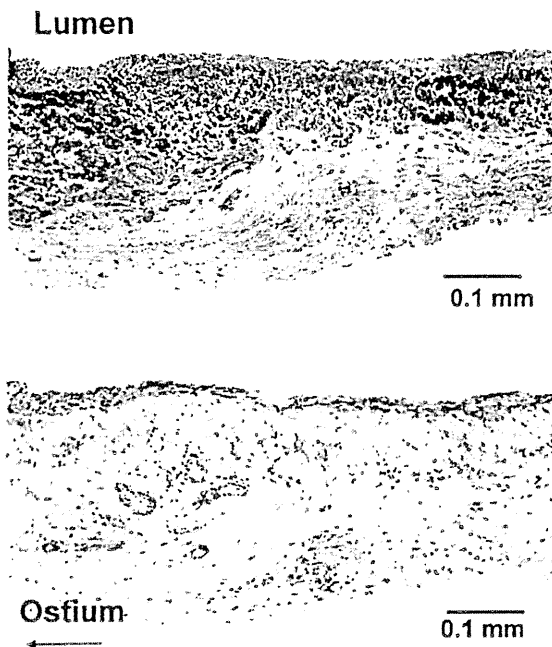


Fig. 1. Photomicrographs of longitudinal sections of the left superior pulmonary vein of the guinea pig. Upper panel: masson trichrome staining. Lower panel: immunostaining for  $\alpha$ -smooth muscle actin ( $\alpha$ -SMA)

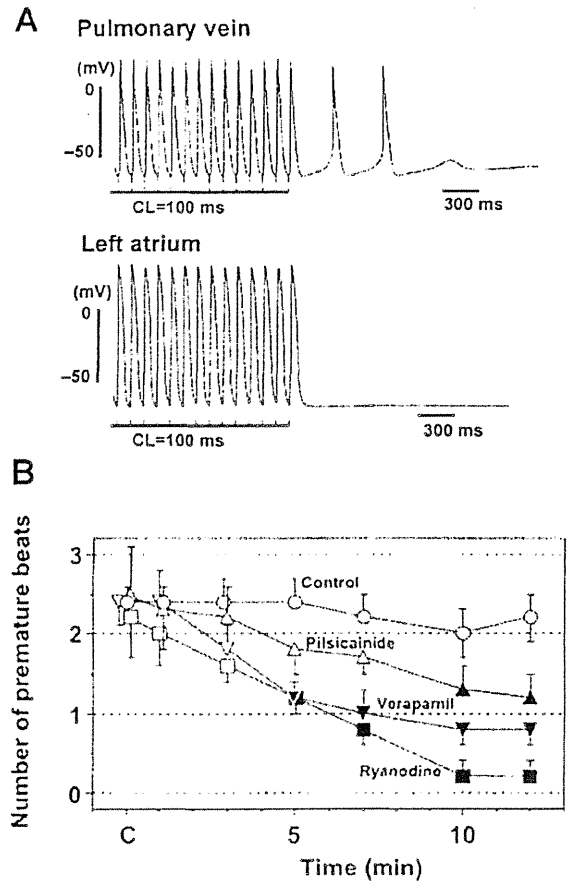


Fig. 2. Delayed afterdepolarization (DAD)-related triggered activity induced by train stimulation. A: A typical tracing of DAD-related triggered activity recorded from the pulmonary vein myocardium after the train stimulation at a pacing cycle length of 100 ms. Two premature beats were detected in this preparation. The DAD-related triggered activity was not observed in the left atrium. B: Summary of the effects of pilsicainide, verapamil, and ryanodine on the number of premature beats in the pulmonary vein preparation. Train stimulation (CL = 100 ms) was applied to the preparation before (C) and at 1, 3, 5, 7, 10, and 12 min after the drug administration. Data are means  $\pm$  S.E.M. Pilsicainide:  $10 \mu\text{M}$  ( $n = 6$ ), verapamil:  $1 \mu\text{M}$  ( $n = 5$ ), ryanodine:  $0.1 \mu\text{M}$  ( $n = 5$ ), and control ( $n = 5$ ). Closed symbols represent significant differences from the corresponding pre-drug values (C) at  $P < 0.05$ . CL = cycle length.

Table 1. Frequency-dependent induction of the triggered activity in pulmonary vein

Pacing cycle length	Pulmonary vein			Left atrium
	200 ms	150 ms	100 ms	100 ms
Incidence	18/45 (40.0%)	33/45 (73.3%)	43/45 (95.6%)	0/8 (0%)
Number of premature beats	$0.7 \pm 0.1$	$1.4 \pm 0.2^*$	$2.1 \pm 0.2^*$	$0 \pm 0$
Coupling interval (ms)	$613 \pm 24$	$564 \pm 18$	$490 \pm 16^*$	—

Data are means  $\pm$  S.E.M. \* $P < 0.05$ , compared with the corresponding values at a pacing cycle length of 200 ms.

among the groups. The number of triggered activity was unchanged during the observation period in the absence of drugs (control), whereas it was significantly decreased by pilsicainide at 10  $\mu$ M, verapamil at 1  $\mu$ M, and ryanodine at 0.1  $\mu$ M, as shown in the Fig. 2B.

#### Effects of carbachol on the triggered activity

At the pre-drug period, the number of triggered activity was  $2.2 \pm 0.5$  in the carbachol group. Carbachol at 0.3  $\mu$ M decreased the number of triggered activity, as shown in the Fig. 3. The same concentration of carbachol shortened the action potential duration of the left atrium electrically driven at 1 Hz without affecting the resting membrane potential, as shown in Table 2. On the other hand, carbachol shortened the action potential duration of the pulmonary vein myocardium together with significant hyperpolarizing effects on the resting membrane potential.

#### Discussion

In this study, we investigated the inducibility of triggered activity in the guinea-pig pulmonary vein myocardium, which is distributed at the mid-layer of the pulmonary vein tissue, as shown in Fig. 1. The shorter pacing cycle length (100 ms) of train stimulation provoked triggered activity in the pulmonary vein preparation, whereas such phenomenon was not observed in the left atrial preparations (Fig. 2A). In previous studies using isolated ventricular tissues, triggered activity is often induced by train stimulation in the presence of intracellular  $Ca^{2+}$  overload by using cardiac glycoside or low  $K^+$  / high  $Ca^{2+}$  extracellular solution (10, 12, 15). In this study, however, the triggered activity could be induced in the pulmonary vein preparation under the normal experimental condition consisting of a standard physiological solution without cardiac glycoside, as shown in Fig. 2A. These results suggest that the pulmonary vein prepara-

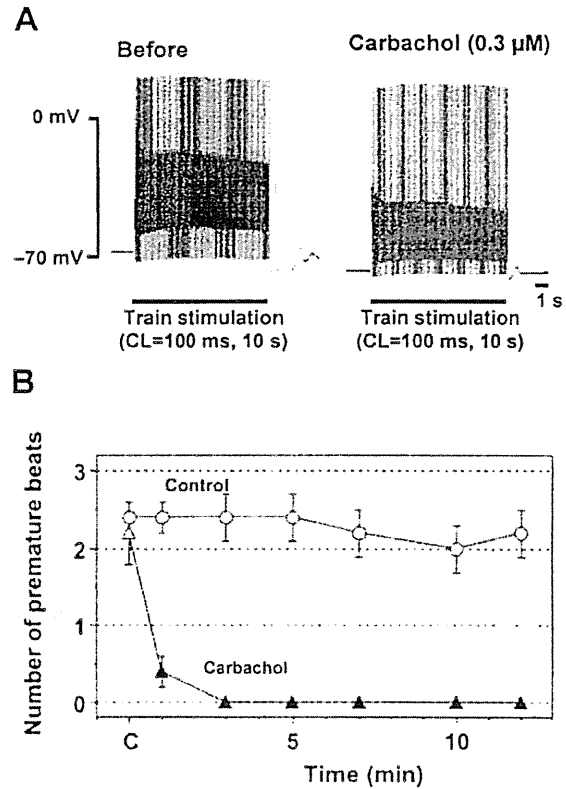


Fig. 3. Effects of carbachol on the DAD-related triggered activity elicited in the pulmonary vein preparation. A: Typical tracings of effects of carbachol on the DAD potentials after the train stimulation at a pacing cycle length of 100 ms. B: Summary of the effects of carbachol (0.3  $\mu$ M,  $n = 5$ ) on the number of premature beats. Train stimulation (CL = 100 ms) was applied to the preparation before (C) and at 1, 3, 5, 7, 10, and 12 min after the drug administration. Data are means  $\pm$  S.E.M. Closed symbols represent the significant differences from corresponding pre-drug values (C) by  $P < 0.05$ .

Table 2. Effects of carbachol (0.3  $\mu$ M) on the action potential parameters of the pulmonary vein and left atrium

	Pulmonary vein		Left atrium	
	Before	Carbachol	Before	Carbachol
RP (mV)	$-70.3 \pm 1.0$	$-75.4 \pm 0.9^*$	$-80.6 \pm 1.1$	$-80.0 \pm 0.6$
OS (mV)	$27.9 \pm 2.3$	$26.4 \pm 1.4$	$27.1 \pm 0.8$	$18.2 \pm 1.4^*$
APD <sub>20</sub> (ms)	$13.2 \pm 0.6$	$9.8 \pm 0.5^*$	$23.3 \pm 1.2$	$12.7 \pm 0.8^*$
APD <sub>50</sub> (ms)	$28.0 \pm 1.9$	$18.9 \pm 1.1^*$	$40.7 \pm 1.6$	$21.3 \pm 1.1^*$
APD <sub>90</sub> (ms)	$75.5 \pm 2.5$	$57.6 \pm 3.5^*$	$76.1 \pm 2.7$	$45.5 \pm 1.9^*$

Data are means  $\pm$  S.E.M. of 5 experiments. The preparations were electrically driven at 1 Hz. Resting potential (RP); overshoot (OS); action potential duration at 20% (APD<sub>20</sub>), 50% (APD<sub>50</sub>), and 90% (APD<sub>90</sub>) repolarization. \* $P < 0.05$ , compared with the corresponding control values (Before).